

CHALMERS



The influence of track stiffness on rail crack occurrence

Projet de Fin d'Études en Génie Mécanique

MALLORIE SEGOND
QUENTIN WIBAUX

Department of Applied Mechanics
Division of Dynamics
CHALMERS UNIVERSITY OF TECHNOLOGY
Gothenburg, Sweden 2014

PROJET DE FIN D'ÉTUDES EN GÉNIE MECANIQUE

The influence of track stiffness on rail crack occurrence

MALLORIE SEGOND

QUENTIN WIBAUX

Department of Applied Mechanics
Division of Dynamics
CHALMERS UNIVERSITY OF TECHNOLOGY
Gothenburg, Sweden 2014

The influence of track stiffness on rail crack occurrence
MALLORIE SEGOND, QUENTIN WIBAUX

© Department of Applied Mechanics, 2014

Projet de Fin d'Études
Department of Applied Mechanics
Division of Dynamics
Chalmers University of Technology
SE-412 96 Gothenburg
Sweden
Telephone: + 46 (0)31-772 1000

Chalmers reproservice / Department of Applied Mechanics
Gothenburg, Sweden 2014

The influence of track stiffness on rail crack occurrence
Projet de Fin d'Études en Génie Mécanique
MALLORIE SEGOND, QUENTIN WIBAUX
Department of Applied Mechanics
Division of Dynamics
Chalmers University of Technology

ABSTRACT

To predict crack growth in railway rails, measurements of track characteristics have been post-processed. Potential correlation between track parameters (e.g. longitudinal level, deflection and track stiffness), and defect positions as detected by ultrasonic testing of rails has been investigated. Although no straightforward correlation was found there were indications of stiffness variations in connection to detected cracks.

A deeper investigation was realized regarding measured track stiffness and deflections around detected defects. Deviations of these parameters at detected defect locations were found. However not all defects could be linked to significant deviations (and vice versa).

A further study was carried out on the influence of hanging sleepers. These will cause track stiffness variations, which will increase the bending moment in the rail and may promote growth of rail cracks. Results of the studies carried out specify a distance over which the bending moment is increased. This affected length surrounding hanging sleepers should be investigated during maintenance operations to detect potential rail cracks and thereby avoid subsequent rail breaks.

Finally, the report outlines a procedure for how measured track stiffness can be included in an analysis of resulting rail bending moments. Thereby track sections with an increased risk of rail crack growth may be detected and mitigated.

Spårstyvhetens inverkan på sprickbildning i räler
Avslutande projekt inom Génie Mécanique
MALLORIE SEGOND, QUENTIN WIBAUX
Institutionen för tillämpad mekanik
Avdelningen för Dynamik
CHARMEC
Chalmers tekniska högskola

SAMMANFATTNING

Spårstyvhetsmätningar har analyserats för att undersöka eventuell korrelation med detekterade rälsprickor. Trots att variationer i spårstyvhet ofta kunde identifieras i närheten av detekterade sprickor kunde ingen tydlig korrelation fastställas.

En mer detaljerad undersökning gjordes med avseende på uppmätt spårstyvhet och nedböjning vid detekterade sprickor. Studien identifierade variationer i dessa parametrar vid detekterade sprickor. Dock kunde inte alla defekter kopplas till signifikanta variationer (och vice versa).

En ytterligare studie genomfördes av inverkan av hängande sliprar. Dessa orsakar spårstyvhetsvariationer vilka ökar det böjande momentet i rälen, vilket i sin tur kan leda till snabbar spricktillväxt. Analysen identifierade ett avstånd över vilket böjmomentet ökade. Detta intervall runt slipern bör identifieras vid underhåll för att detektera eventuella sprickor och därmed undvika framtida rälsbrott.

Slutligen demonstrerar rapporten hur uppmätta spårstyvheter kan inkluderas i en analys för att fastställa böjmomentfördelning längs rälen. Därigenom kan sektioner med förhöjd risk för rälsprickor identifieras och åtgärdas.

Nyckelord: Järnvägsmekanik, spårstyvhet, rälsprickor, rälsbrott

Contents

ABSTRACT	I
SAMMANFATTNING	II
CONTENTS	III
PREFACE	V
1 INTRODUCTION	1
2 ABOUT EBER DYNAMICS	2
3 THEORETICAL BACKGROUND	3
3.1 Measurement methods and database	3
3.2 Track stiffness/defection and track degradation	4
3.3 Track stiffness and hanging sleepers	5
4 METHOD	6
4.1 Track stiffness and rail defects correlation	6
4.1.1 Pre-processing of stiffness measurement data	6
4.1.2 Analysis of track characteristics at detected defects	7
4.1.3 Analysis of correlation between detected cracks and local track stiffness deviations	8
4.2 Finite elements simulations of bending moments in the vicinity of hanging sleepers	8
5 RESULTS	11
5.1 Correlation between measured track stiffness and detected rail defects	11
5.1.1 Analysis of track characteristics at detected defects	11
5.1.2 Analysis of correlation between detected cracks and local track stiffness deviations	16
5.1.3 Analysis of filtered deflection deviations around detected defects	20
5.2 Finite elements simulations of bending moments in the vicinity of hanging sleepers	21
5.2.1 General comments on results	21
5.2.2 One hanging sleeper	22
5.2.3 Several hanging sleepers	25
5.2.4 Variation of the input parameters	27
5.2.5 Application with real stiffness values (from measurement database)	29
6 CONCLUSION	31
7 RECOMMENDATIONS	32

8	REFERENCES	33
9	APPENDICES	34
9.1	MATLAB code for analysis of track characteristics at detected defects	34
9.2	MATLAB code for local track stiffness deviations	37
9.3	ANSYS command file for estimating bending moments in a rail with hanging sleepers	40
9.4	Track characteristics extracted from sample 1 for four detected defects	44
9.5	Track stiffness deviations of samples 2 to 5	48
9.6	Deviations of deflection with short wavelength content of samples 2 to 5	51
9.7	Maximum and minimum bending moments along the rail considering several hanging sleepers	53
9.8	Maximum and minimum bending moments along the rail with different loads and nominal stiffness	55

Preface

This Master's thesis has been carried out at Chalmers University of Technology, in the department of Applied Mechanics. The work has been performed in collaboration with EBER Dynamics in Chalmers' facilities from the 20th January 2014 to the 3rd of June 2014.

First of all, we would like to express our sincerest gratitude to Anders Ekberg, Professor at Chalmers University of Technology and Director of CHARMEC (Chalmers Railway Mechanics), who supervised our work at Chalmers, for his support, remarks and advices.

In addition, we would like to express our appreciation to our supervisor at EBER Dynamics, Eric Berggren, for proposing this work and to being able to answer our questions in a quick and efficient way in spite of the distance.

Our thanks also go to Carina Schmidt and Ing-Britt Carlsson for all their administrative support.

Last but not least, we would like to thank Chalmers University of Technology, and more especially the department of Applied Mechanics, for allowing us to perform this Master's thesis project as part of our academic exchange.

Göteborg June 2014

Quentin Wibaux, Mallorie Segond

1 Introduction

Rail cracks can lead to rail breaks and therefore potentially to operational delays and accidents. To avoid this, track measurements are carried out in order to predict required maintenance operations. However, it is currently difficult to detect from measurements which defects are critical from a maintenance point of view. The current study is mainly focused on track stiffness and hanging sleepers, as the latter can be seen as an extreme case of track stiffness variations.

Problems which have been identified are the following:

- How, to anticipate the apparition of cracks and the maintenance operations to fix them from track stiffness/deflection measurements?
- What is the influence of hanging sleepers – as an extreme case of track stiffness variations – on the bending moment in the rail?

The first part of the project is to investigate whether a correlation exists between track parameter variations (track stiffness, deflection, longitudinal level) extracted from new measurement method developed by EBER Dynamics (see part 2), and cracks identified by ultrasonic testing of rails. This correlation analysis is performed using MATLAB.

Hanging sleepers lead to a local decrease of stiffness, and thereby to an increase of the bending moment in the rail that promotes rail crack growth. Consequently, studying the location of hanging sleepers, or track stiffness variations, should indicate critical zones regarding rail defects. However, track stiffness deviation is not the only driving force that leads to rail cracks. Indeed, wheel/rail friction, contact stresses or rail material resistance which may vary along the rail can also promote crack formation and growth. Hence, it is not expected that all detected cracks occur in the vicinity of a hanging sleeper, but it is expected that the occurrence of hanging sleepers locally increases the risk of rail cracks.

Secondly, the influence of an increased bending moment, due to the larger deflection at hanging sleepers will be studied. Results from these studies will aid in the prediction of maintenance needs and the prevention of rail breaks. The objective of the second part is to quantify the influence of a larger bending moment due to hanging sleepers. Here finite elements simulations featuring ANSYS are employed. The point is to identify the affected area surrounding a hanging sleeper where bending moments are increased. This would identify the limits of the influence of the hanging sleeper and thereby the extent of the region that would require more in-depth inspections for potential cracks.

2 About EBER Dynamics

Created in 2010, EBER Dynamics is a company specialized in the field of railway track measurements. In partnership with many companies and universities, such as Chalmers University of Technology and CHARMEC (Chalmers Railway Mechanics), it offers different services like:

- Track stiffness and deflection measurements, thanks to two new innovative patented measurement systems,
- A new continuous method to monitor stress free temperature in order to prevent track buckling (still in progress),
- Measurement services, to help monitoring different aspects of railway (production measurements, measurement system development and software development),
- Consultancy for analyzing measurement data.

Therefore the main goal of EBER Dynamics is to realize and study a range of measurements on railway tracks to prevent dangerous defects and predict maintenance operations. These defects can lead to rail or wheel cracks but also to breaks and unacceptable accidents. To prevent this, EBER Dynamics has already collected and studied a large amount of data (obtained with its new measurement method) to link track stiffness/deflection to the longitudinal level, with the aim of giving indication of a fast degrading track. These studies indicated a link between large deflections and track degradation, but did not permit to find a simple connection between stiffness/deflection and the evolution of the longitudinal level.

In addition, ranges of measurements realized with ultrasonic's technology has been collected and enable to detect and classify defects according to different criteria such as the priority of the defect.

More information about EBER Dynamics can be found on the webpage <http://www.eberdynamics.se>.

3 Theoretical background

3.1 Measurement methods and database

One part of the current project is to determine if there exists a correlation between the position of detected rail cracks and track mechanical parameters such as track stiffness, track deflection or longitudinal level. To do so, two different measurement databases are used:

- Measurements obtained with EBER Dynamics' new method which provide track mechanical parameters,
- Measurements obtained by ultrasonic testing of rails, giving the position and categorization of identified defects.

The method developed by EBER Dynamics, called EBER Vertical Stiffness (EVS) enables to calculate track stiffness and deflection based on measured longitudinal level. Track longitudinal level is measured by two different techniques of measurements: inertial measurements and chord based systems. By comparing these, deflection is obtained as well as the stiffness when the wheel contact force is estimated with a simulation program (see [1]). The principle is based on the fact that the longitudinal level s_L measured under a loaded axle is composed of an unloaded longitudinal level s_U (due to track irregularities) and a load contribution w that can be assessed from deflection in x due to a load in x_1 :

$$s_L(x) = s_U(x) + w(x, x_1)$$

The goal of the method is then to derive w . The detailed method used to calculate the deflection is described in [1]. EVS is an innovative method as it gives the possibility to monitor the longitudinal level and track stiffness under a loaded axle at the same time using a track recording car. EVS also differs from the old principle, the Rolling Stiffness Measurement Vehicle (RSMV), by being closer to the normal traffic condition since the EVS gives a response similar to a passing train.

The self-propelled track recording car used for the current measurements is the IMV100 (Infranord Measurement Vehicle 100 km/h), operated by Infranord in Sweden. The Iron-ore line links Luleå to Riksgränsen in northern Sweden, and connects to Narvik on Ofotenbanen with a distance of 473 km, and is mainly operated by heavy freight trains with a maximum axle load of 30 tonnes. The line is divided in three major track sections, 111, 113 and 118, and four additional track sections, 112, 116, 114 and 119. The project focuses on the section 118 (Boden–Gällivare) of the Iron-ore line.

The longitudinal level is usually recorded at least four times per year on the Iron-ore line. For the EVS project a special order of measurements was done. Measurements were performed in February, April and August of 2012 and in November 2013 (to assess the influence of the seasonal temperature). In the provided database, the samples were performed on the following dates:

- Sample 1: 25th of April 2012,

- Sample 2: 29th of April 2012,
- Sample 3: 15th of February 2012,
- Sample 4: 14th of August 2012,
- Sample 5: 6th of November 2013.

The database used in this project is thereby composed of five samples all corresponding to the section 118 and containing:

- The position in km (distance from a reference position),
- Coordinates following the SWEREF99 system,
- The longitudinal level of the left and right rail in mm,
- The curvature in m^{-1} ,
- The speed of the track recording car in km/h,
- The mean track deflection of the left and right sides in mm,
- The mean track stiffness of the left and right sides in kN/m,
- The track deflection of left and right rail, filtered at short wavelength.

In addition, it is possible to filter the longitudinal level at any frequency band.

The second database is provided by Trafikverket and includes defects detected by ultrasonic testing from 2010 to 2013. Here the defect ID, the inspection date, the track section, the defect position, the UIC code of the defect and the defect classification are reported.

The UIC Code, following [2], identifies the type of rail defects.

The classification indicates the priority/severity of the defect and can be stated as 1a, 1v, 1m, 2 or 3, with the following meaning:

- 1 means it should be fixed within the time defined by the letter a (immediate), v (week) or m (month),
- 2 or 3 means the defect is registered but left in track as there is no safety problem.

3.2 Track stiffness/deflection and track degradation

EBER Dynamics has made a study (see [1]) on a potential correlation between track stiffness / deflection and track degradation, focusing on the iron-ore line and especially the section 118.

Firstly it has been shown that the seasonal temperature variations do not have a strong influence on the track displacement and longitudinal level. Whereas the mean value of the static displacement slightly differs between seasons, the mean for longitudinal level does not vary.

A second part studied the evolution in time of longitudinal level and deflection. This analysis shows that both parameters can indicate a degrading track, with a local increase of their amplitude or top-to-top values over the years. When trying to link

track deflection with longitudinal level a linear correlation exists for wavelengths 3–9 meters and 1–25 meters although scatter can be found. For wavelengths in the interval 1–4 meters, the correlation is not that clear and a larger scatter is observed. The aim of establishing the correlation is to give early indications of fast degrading tracks. This could be done by setting a limit value for deflection with respect to longitudinal level. However, such a limit cannot be applied for now as the link between deflection and longitudinal level cannot be sufficiently clearly defined at this stage.

3.3 Track stiffness and hanging sleepers

Track stiffness is an important parameter regarding the wheel/rail contact and therefore track quality. Although a too high or too low stiffness is not good for the track, it is to an even higher extent that stiffness variations must be taken into consideration. As explained in [3] track stiffness stands for the stiffness of the entire system of rail, sleepers, ballast and sub-layers (see Figure 1). Hanging sleepers, which are sleepers not supported or partially supported by the ballast, can be seen as short wavelength stiffness variations. However a short wavelength stiffness variation does not automatically imply a hanging sleeper, it may also be, for instance, an insulating joint.

Different kinds of simulations have been developed and reported in [4] calculating the bending moment of the rail when considering a hanging sleeper. Each sleeper is here modeled by a spring and is thus introduced as a reduced stiffness. It has been shown that for a pure hanging sleeper (no stiffness at all) the bending moment is increased by 60% of the value without a hanging sleeper.

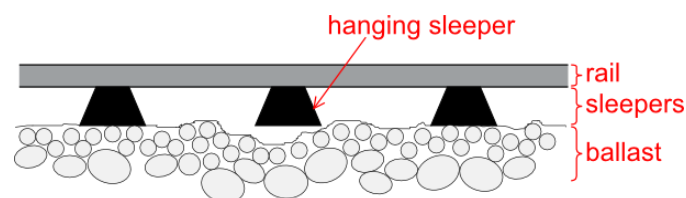


Figure 1 - Section of a rail supported by sleepers and ballast

4 Method

4.1 Track stiffness and rail defects correlation

The measurements provided by EBER Dynamics and the database of ultrasonic testing of the rails are used for the correlation study. The way these two databases have been obtained is detailed in the section 3.1.

To study if a correlation exists, different steps have been undertaken with MATLAB:

- Pre-processing of stiffness measurement data,
- Analysis of track stiffness characteristics at detected defects,
- Analysis of correlation between detected cracks and local track stiffness deviations.

4.1.1 Pre-processing of stiffness measurement data

It has been noticed that, when plotting the longitudinal level, deflection or stiffness with respect to the position along the track (see section 4.1.2 below) that unexpected peaks can appear, usually rather far from the location of any defect. These large amplitude peaks are not related to the real longitudinal level, deflection or track stiffness, but can be explained by a too low velocity of the track recording car. As the track recording car velocity tends to zero (i.e. if the vehicle travels at low speed or stops), the monitored longitudinal level (and therefore the deflection) will be subjected to numerical errors, due to the double integration of acceleration involved in the evaluation.

To avoid this kind of peak values and disturbances, one solution is to change the values of the studied parameter (longitudinal level, deflection or stiffness) when the recording car velocity decreases below a chosen limit. This velocity limit is in the current study taken as 10 km/h but can easily be modified. Values of the studied parameters at these low speeds are set to an average value calculated over the whole sample of the studied track section (see 3.1).

A significant drawback is the case where a defect is located on a part of the rail where the track recording car has a low velocity. As the recorded parameters are disturbed and thus set to an average value these defects cannot be related to any deviations in track stiffness, longitudinal level or deflection.

An example of graphs obtained with the consideration of the low velocity is given in Figure 2.

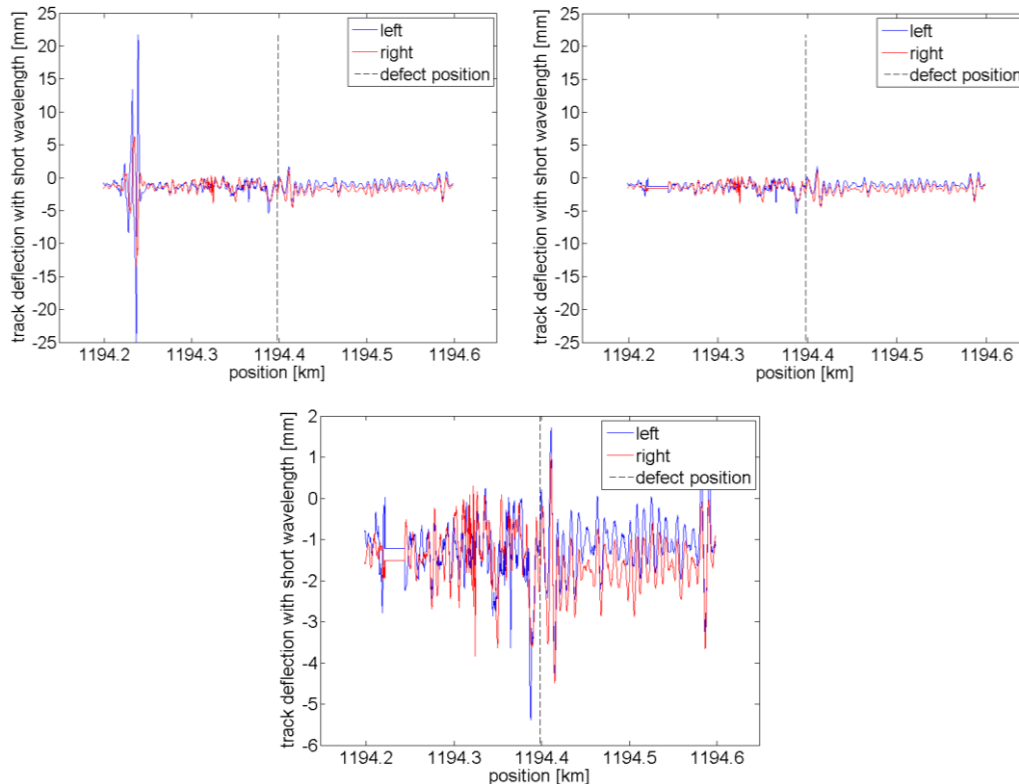


Figure 2 - Top left: Deflection with short wavelength content showing peaks far from a detected defect ; Top right: Deflection with short wavelength content after removing the non-physical peaks ; Bottom: Rescaled deflection with short wavelength content after removing the peaks

4.1.2 Analysis of track characteristics at detected defects

As stated in 3.2 referring to [1], a previous study to find a correlation between longitudinal level and deflection with the aim of predicting fast degrading tracks has been carried out. This previous study did not find any clear-cut correlation. To expand the analysis, further parameters can be investigated:

- Longitudinal level and filtered longitudinal level,
- Track deflection (i.e. static displacement) and filtered deflection,
- Track stiffness.

These parameters will in the current study be connected to the ultrasonic testing of rails and resulting indications of rail cracks. The connection between the two sets of data is the position, which is given as a kilometer distance. However an uncertainty of 20 meters regarding the position must currently be considered due to the lack of precision in the positioning system. The process of evaluating any correlation is the following:

- A detected defect is selected in the database containing results from ultrasonic testing and its location is employed as an input parameter in the MATLAB command file,
- The sample to be analyzed is selected, i.e. the recording date (February 2012, April 2012, August 2012 or November 2013),

- The parameter to be studied is chosen (longitudinal level, deflection, stiffness),
- Plot magnitude(s) of studied parameter(s) as a function of position along the rail in the vicinity of the defect.

The MATLAB code is available in Appendix 9.1.

4.1.3 Analysis of correlation between detected cracks and local track stiffness deviations

As mentioned in section 3.3, hanging sleepers promote a locally low stiffness (and stiffness variations), whereas the opposite is not always true (a low stiffness is not automatically due to the presence of hanging sleepers). The subsequent part of the analysis aims at computing the ratio of minimum stiffness k_{\min} over nominal stiffness k_{nom} .

The following steps have been applied:

- Stiffness magnitudes from the measurement database are pre-processed to remove peaks caused by low velocity of the recording car,
- For one defect, the minimum stiffness around this defect ($\pm l_{\min}$) is stored as k_{\min} ,
- For the same defect, the mean stiffness is calculated at a distance ($\pm l_{\text{nom}}$) around the defect and stored as k_{nom} ,
- The ratio k_{\min}/k_{nom} is calculated.

l_{\min} is a short distance that accounts for the uncertainty of the measured position in the ultrasonic database and the measured position in the stiffness/deflection database. For the current analysis l_{\min} is set to 20 meters. l_{nom} is taken large enough to represent the nominal characteristics of the track section around the defect. In the current study l_{nom} is taken as 100 meters.

A ratio close to 1 indicates that there is no stiffness variation at the location of the detected defect. In contrast, a ratio much lower than 1, corresponds to a stiffness variation caused e.g. by soil variations.

The MATLAB code is available in Appendix 9.2.

4.2 Finite elements simulations of bending moments in the vicinity of hanging sleepers

Finite elements simulations have been carried out with ANSYS Mechanical APDL 14.5. One can refer to the command file for the details, see Appendix 9.3.

The model includes one 20-meter long rail, modeled as a beam following the Timoshenko beam theory. The beam is supported by sleepers directly linked to the ground, and represented by springs (one spring per sleeper) with a nominal stiffness, k . Hanging sleeper(s) have a reduced stiffness, k' (or no stiffness at all), as shown in

Figure 3. The expressed stiffness corresponds in fact to the ballast stiffness (we consider sleepers as rigid bodies). The stiffness for the hanging sleeper(s) is expressed as a percentage of the nominal stiffness. The rail is loaded with four vertical loads, corresponding to four wheels. The axle load is divided by two as only one rail is considered.

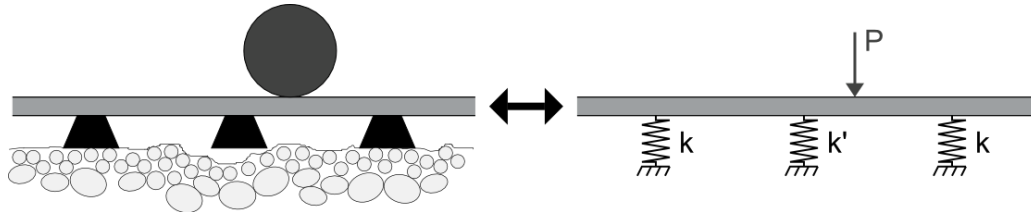


Figure 3 - Mechanical equivalent scheme of the rail supported by sleepers represented by springs of stiffness k and k' for the hanging sleeper, and a passing wheel of load P

The parameters for the initial model are:

- Nominal stiffness: 50 MN/m
- Axial load: 25 tonnes
- Stiffness for the hanging sleeper(s): 0%, 25%, 50% or 75% of the nominal stiffness

These parameters are fixed for the initial model but their variation will be considered.

Geometrical values:

- Span between two sleepers: 65 cm
- Span between the first and the second wheels: 1.80 m
- Span between the second and third wheels: 3.20 m
- Span between the third and fourth wheels: 1.80 m
- Cross-sectional area: 76.7 cm² (norm EN13674-1)
- Area moment of inertia around the y-axis: 512.3 cm⁴ (norm EN13674-1)
- Area moment of inertia around the z-axis: 3038.3 cm⁴ (norm EN13674-1)
- Torsional constant: 3.048.10⁻⁵ m⁴
- Thickness along y: 172 mm (norm EN13674-1)
- Thickness along z: 150 mm (norm EN13674-1)

The span between sleepers is chosen in accordance with the standard length. The span between the wheels is representative for a freight train of axial load 25 tonnes.

Material properties:

- Young modulus of the material: 210 GPa
- Poisson coefficient: 0.3
- Density: 7862 kg/m³ (norm EN13674-1)

The element types chosen for the model are BEAM188 (linear – 2 nodes) for the rail and COMBIN14 (spring–damper combination) for the sleepers.

Boundary conditions are:

- Fixed support ($u_x = u_y = u_z = 0$) on the left end of the beam

- Movable support ($u_y = u_z = 0$) on the right end of the beam
- Clamping (all degrees of freedom equal zero) of the bottom end of the springs
- 4 loads of 12.5 tonnes (for 25 divided by two) – the influence of the load will be considered

Different configurations of hanging sleepers are studied:

- 1 hanging sleeper at position 9.75 m
- 2 consecutive hanging sleepers at positions 9.75 and 10.4 m
- 2 hanging sleepers separated by a normal sleeper, at positions 9.1 and 10.4 m
- 3 consecutive hanging sleepers at positions 9.1 , 9.75 and 10.4 m

Recall that the rail length is 20 meters, which means that the studied hanging sleeper(s) are roughly located in the middle.

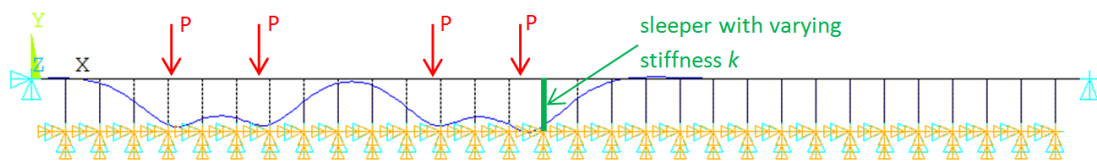


Figure 4 - Boundary conditions and deformed rail (blue)

As we need to simulate the four wheels passing on the rail, the program sets out from an initial position of the wheels. The position is then incremented forward along the rail so that the wheels pass each node. At each step (corresponding to a given position of the wheels), a quasi-static analysis is carried out and bending moments and deflections of the rail are evaluated.

5 Results

5.1 Correlation between measured track stiffness and detected rail defects

The model is described in the section 4.1.

5.1.1 Analysis of track characteristics at detected defects

As explained previously, the aim of this part of the study is to link the two databases containing locations of detected defects and measured track stiffness. For a given defect, rail characteristics (stiffness, track deflection, longitudinal level, ...) in the vicinity of the defect are plotted for the left and right rail (blue and red lines, respectively in the following graphs). In this manner an overview of the variations of these characteristics is obtained. Both left and right rails are considered since it is not mentioned in which rail defects are detected.

More than 700 000 measured values have been recorded per measurement sample (5 samples in total – see 3.1 for the description of the samples). Consequently there is a massive amount of results that can be analysed. To facilitate data processing, only the first sample (April 2012) will be analysed in detailed here. A further study that was performed on the other samples led to the same conclusions.

In Figure 5 track deflections at positions corresponding to selected defects are plotted. Positions of defects given by the ultrasonic testing database are represented by a dashed vertical line. Recall that there may be a difference of maximum 20 meters between positions given by the ultrasonic testing of rails and track stiffness/deflection measurements.

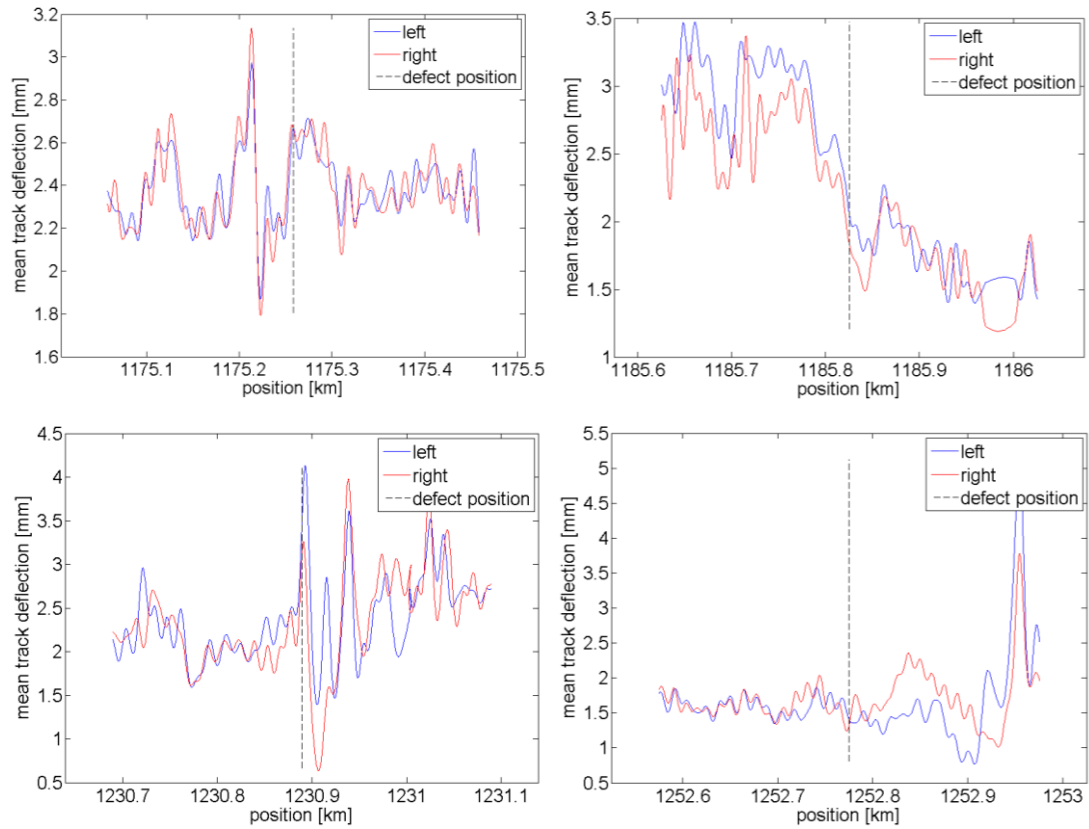


Figure 5 - Track deflection around detected defects located at 1175.258 km (top left), 1185.825 km (top right), 1230.889 km (bottom left), 1252.775 km (bottom right)

Figure 5 shows that for some defects (defects at 1175.258 km, 1185.825 km and 1230.889 km) there is a noticeable variation of the mean deflection at a location close to the defect position. In contrast, for the defect located at 1252.775 km, no significant variation of the mean deflection around the defect can be visualized.

The longitudinal levels in the vicinity of the recorded defects are plotted in Figure 6.

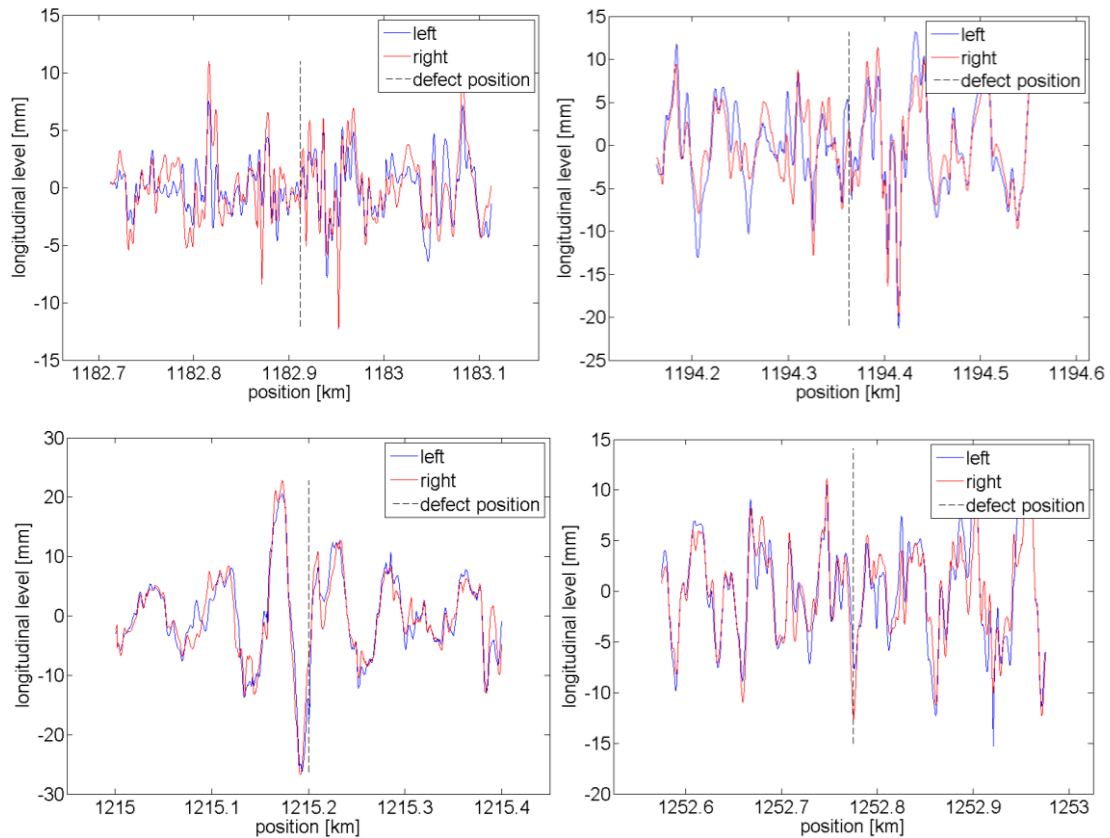


Figure 6 - Longitudinal levels around defects located at 1182.912 km (top left), 1194.363 km (top right), 1215.200 km (bottom left), 1252.775 km (bottom right)

As for the mean track deflection (Figure 5), some plots show a sudden variation of the longitudinal level (defect located at 1215.200 km whereas other defects do not correlate to any clear patterns of variation in longitudinal stiffness).

As illustrated, track deflections and longitudinal levels in the vicinity of a detected defect in some cases show interesting variations. These variations might be linked to the defects though they are not sufficient to identify defects: As shown defects can exist where there is no significant variation of the deflection or longitudinal level (or these may exist but are not sufficiently pronounced to be distinguished from the surrounding variations).

It may be more convenient to look at the deflection or longitudinal level filtered at different wavebands such as 1–25 meters, 3–9 meters or 1–4 meters, in order to compensate for large local variations.

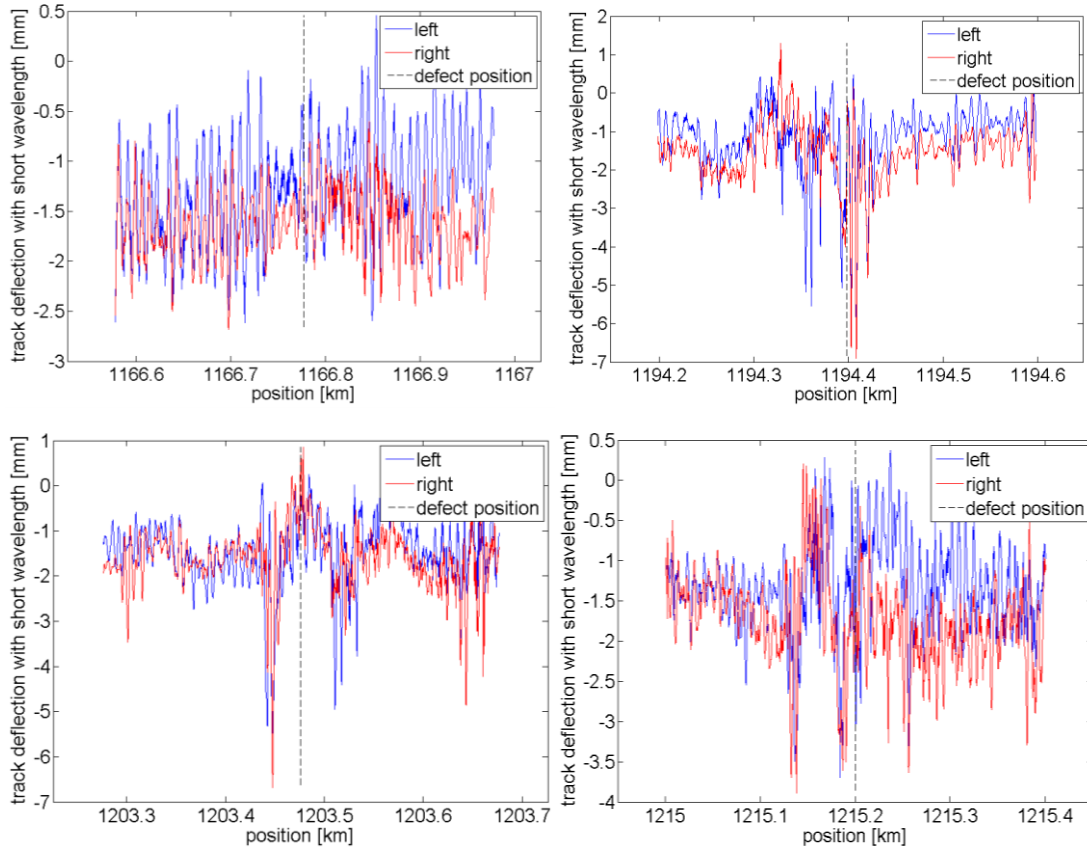


Figure 7 - Track deflection with short wavelength content included plotted around defects located at 1166.777 km (top left), 1194.398 km (top right), 1203.476 km (bottom left), 1215.200 km (bottom right)

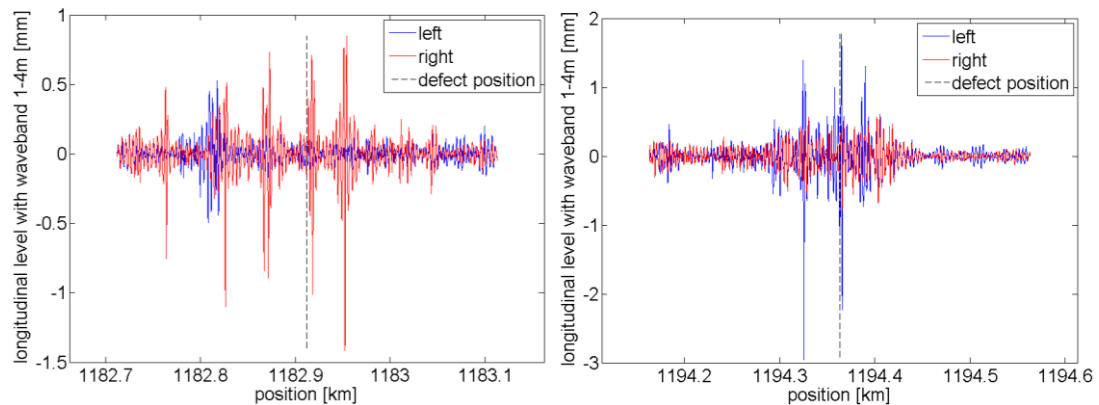


Figure 8 - Longitudinal levels around defects located at 1182.912 km (left) and 1194.363 km (right) filtered at 1–4 m

What is observed in Figure 7 is that the deflection with short wavelength content can be relevant (see defects located at 1194.398 km and 1203.476 km) to identify a defect where there is a noticeable variation at the defect position (or near). This is however not the case for all the defects as shown on the same figure for the two other detected defects.

Longitudinal levels filtered in the waveband 1–4 meters show very sudden peaks (Figure 8). The two cases plotted in Figure 8 correspond to the cases indicated in

Figure 6 for longitudinal level (top left and top right graphs). Whereas in Figure 6 the two corresponding graphs could not indicate clearly the presence of rail cracks, the short wavelength filtered longitudinal level is clearer in indicating the potential existence of a defect. It should however be noted that some peaks are observed although no defect has been detected at the identified position.

Finally, track stiffness in the vicinity of a defect is plotted in Figure 9.

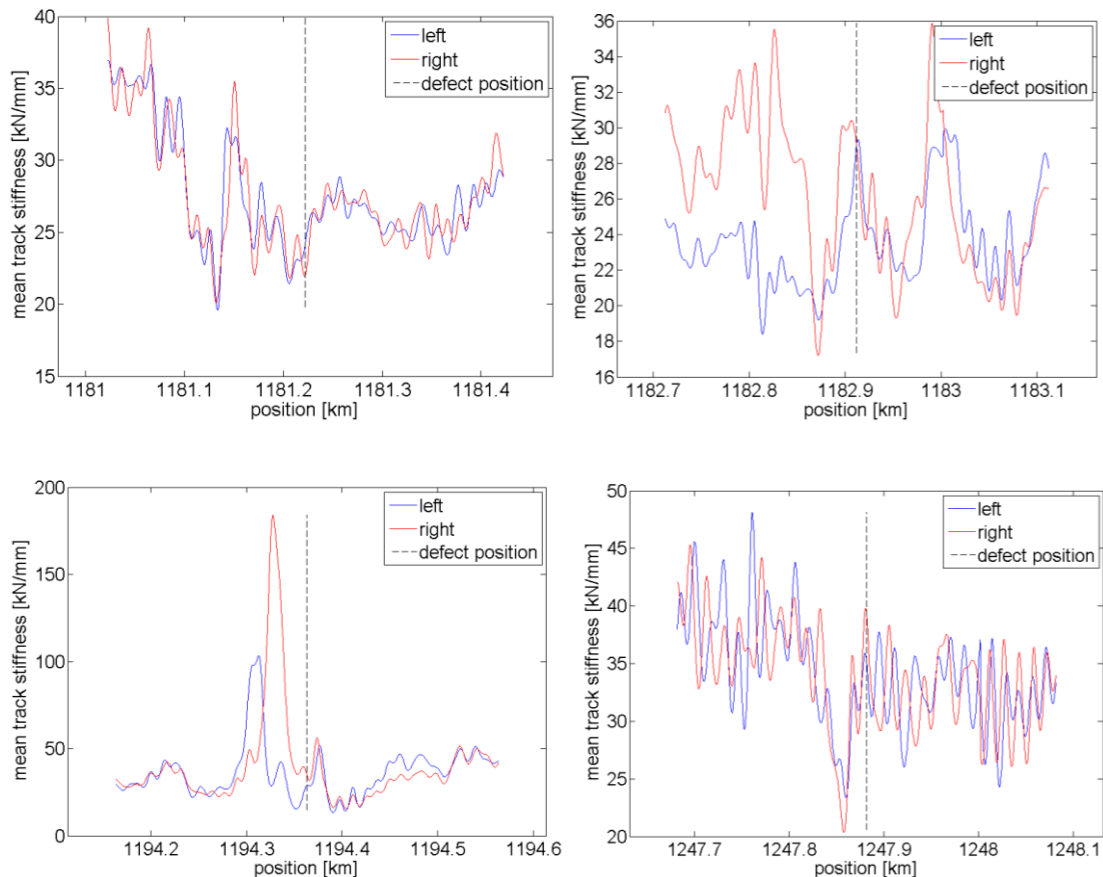


Figure 9 - Track stiffness around defects located at 1181.222 km (top left), 1182.912 km (top right), 1194.363 km (bottom left), 1247.881 km (bottom right)

A study of track stiffness variations around defects leads to the same conclusion as for the other parameters. There are indications that it can be useful as a mean to identify a potential defect (for example the defect at 1194.363 km), but there are not clear patterns in stiffness variations at all locations corresponding to detected defects.

So far different defects have been considered when plotting the deflection, longitudinal level or track stiffness. In Appendix 9.4 all the different parameters for four given defects are presented, in order to investigate if one of those parameters is more relevant regarding the indication of defects. The investigated parameters are: longitudinal level, track deflection, track stiffness, deflection with short wavelength, longitudinal level filtered at 1-25 meters, longitudinal level filtered at 3-9 meters and longitudinal level filtered at 1-4 meters. The four defects have been numbered from (1) to (4). The table in Figure 10 lists parameters showing large magnitudes in the surrounding area of the defect (maximum 20 meters).

Defect number	(1)	(2)	(3)	(4)
Parameters with notable variations	- Track deflection - Track stiffness	- Track deflection - Track stiffness - Longitudinal level 1-4 m	- Longitudinal level - Longitudinal level 3-9 m - Longitudinal level 1-4 m	- Track deflection - Track stiffness

Figure 10 - Parameters with large magnitudes in the vicinity of four defects

It is shown in Figure 10 that none of the studied parameters is implied for all four defects. As a consequence, the investigation of the variations of a given parameter, with the aim of indicating cracks is not straightforward.

Plotting track parameters around defects detected by ultrasonic testing of rails has permitted to investigate if there is a characteristic variation of the studied parameter around defects. After this preliminary study, it seems that it is difficult to draw a general conclusion regarding the correlation between the existence of defects and the evolution of longitudinal level, deflection or track stiffness. Actually, this conclusion could be expected because, even if the presence of hanging sleepers can lead to a local decrease of stiffness, stiffness variations are not the only possible cause of crack formation and growth. Indeed, cracks can also be the consequence of high wheel/rail contact stresses, local stress raisers, locally reduced material resistance etc. However, it should be noted that significant variations of stiffness, deflection or longitudinal level related to the defects are observed in several cases.

There are also many additional aspects that make it difficult to establish a clear link between track parameters and defects:

- Uncertainty of the position of the defect on the order of 20 meters,
- Proximity of several defects: influence of one defect cannot be clearly seen,
- Difference of magnitude of a given parameter, with respect to defects,
- Important variations of track parameters can be more or less spread out around a defect,
- Important variations of track parameters can be mistaken with natural variations.

5.1.2 Analysis of correlation between detected cracks and local track stiffness deviations

In part 5.1.1, the correlation between recorded defects and variations in mechanical characteristics around these defects has been investigated. Defects were chosen arbitrarily among the 145 defects detected on section 118. By following this approach it is difficult to make a general conclusion as the study considers one specific defect at a time (studying all defects of section 118 would lead to 5 samples * 7 characteristics * 145 defects = 5075 graphs), and also due to the different complications listed above.

To improve the analysis of part 5.1.1, this part focuses on the study of stiffness characteristic for all defects recorded on section 118. For simplification only results for sample 1 are presented in this report. Comments on the other samples are provided if necessary.

To study track stiffness deviations at locations of detected cracks, the ratio of minimum stiffness over nominal stiffness, k_{\min}/k_{nom} , has been calculated for all defects, following the method described in 4.1.3. Figure 11 presents this ratio for all defects.

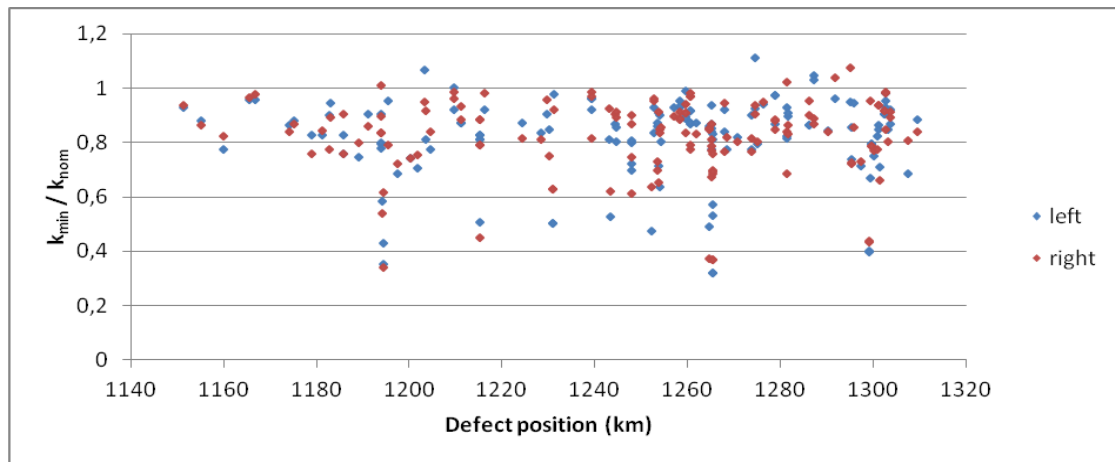


Figure 11 - Track minimum stiffness over nominal stiffness with respect to defect positions for left rail and right rail of sample 1

This figure shows a rather significant scattering of the ratio. In most cases the ratio is included between 0.8 and 1, which means that the minimum stiffness is close to the nominal stiffness and thus there is no large deviation in track stiffness. For a few defects the ratio is below 0.6, meaning that there is a quite significant track stiffness variation in the vicinity of the defect. The table below indicates the number of defects for which the ratio k_{\min}/k_{nom} falls in the given ranges of magnitudes.

	Left rail		Right rail	
	Quantity	%	Quantity	%
$X > 1$	5	3.5	4	2.8
$0.8 < X < 1$	96	67.5	82	56.5
$0.6 < X < 0.8$	27	18.6	51	35.1
$X < 0.6$	15	10.4	8	5.6

Figure 12 - Number of defects with different values of $X=k_{\min}/k_{\text{nom}}$, for the 145 detected defects studied

Figure 11 and Figure 12 show that approximately 90% of defects have a ratio k_{\min}/k_{nom} included between 0.6 and 1.

Examples of stiffness variation around defects, which have a ratio lower than 0.6 are presented in Figure 13.

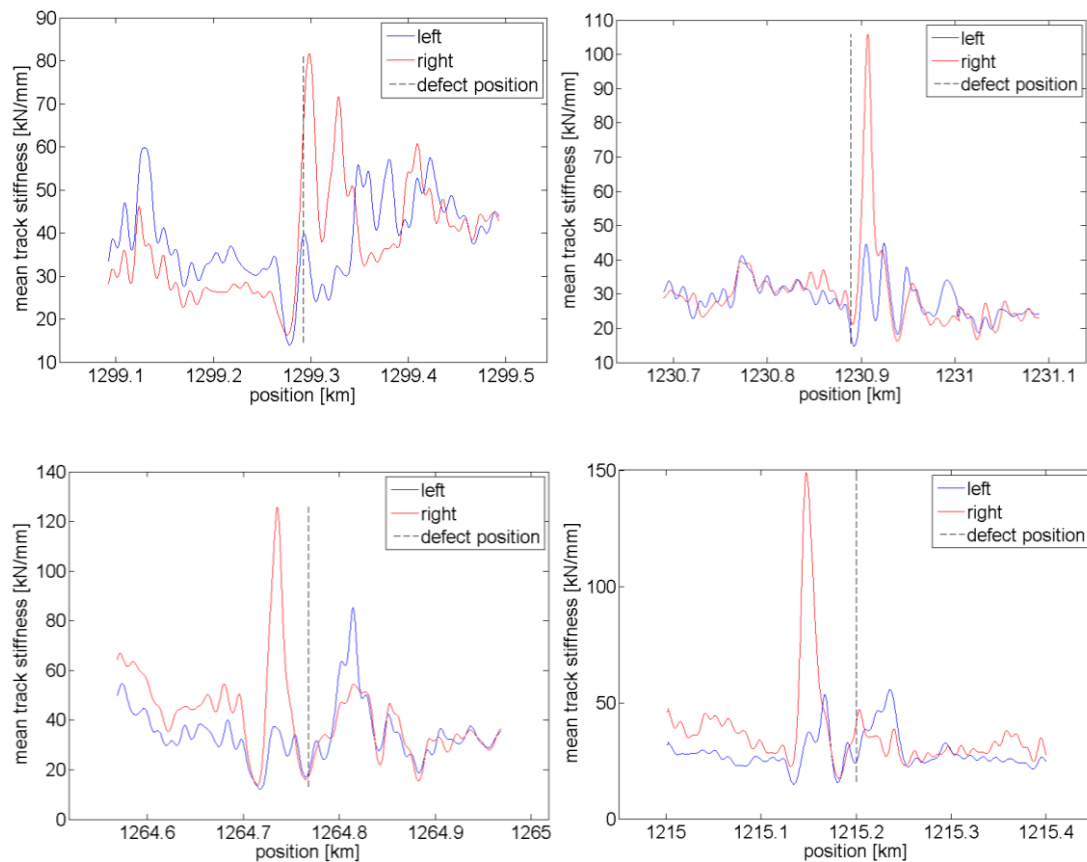


Figure 13 - Track stiffness plotted around defects located at 1299.292 km (top left), 1230.889 km (top right), 1264.768 km (bottom left), 1215.200 km (bottom right)

Figure 13 shows track stiffness variations for four defects with a ratio below 0.6. However all defects in this range have been considered and support these observations. In all cases, a sudden variation of track stiffness is noticeable. Although the studied defects have been selected because of a low value of k_{\min}/k_{nom} , there is always a positive peak, i.e. a maximum value of stiffness, adjacent to the minimum stiffness location. Peak-to-peak stiffness values are consequently large around these selected defects which could be the cause of the defects. The findings encourage a study of the ratio of the maximum stiffness over the nominal stiffness, k_{\max}/k_{nom} , which is presented in Figure 14.

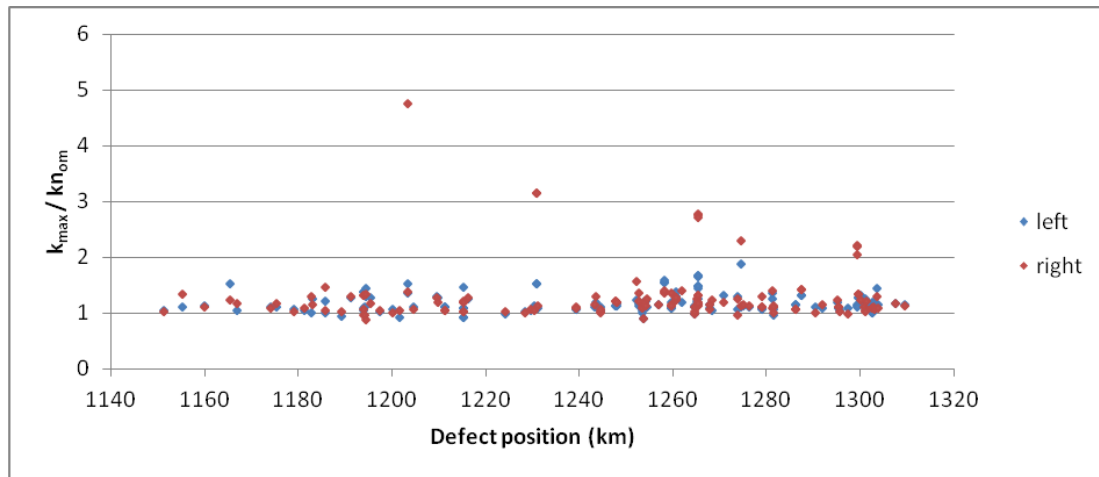


Figure 14 - Track maximum stiffness over nominal stiffness with respect to defect positions for left rail and right rail of sample 1

	Left rail		Right rail	
	Quantity	%	Quantity	%
$X > 2$	0	0	10	6.9
$1.4 < X < 2$	17	11.7	5	3.5
$1.2 < X < 1.4$	31	21.4	39	26.9
$1 < X < 1.2$	88	60.7	83	57.2
$X < 1$	9	6.2	8	5.5

Figure 15 - Number of defects with different values of $X=k_{\min}/k_{\text{nom}}$, for the 145 detected defects studied

Figure 14 and Figure 15 show that only recorded defects on the right rail have a ratio larger than 2. This is in line with observations made in Figure 13 where the right rail has larger increases of track stiffness than the left rail.

For the highest ratios presented in Figure 14, values of maximum stiffness seem to be very high: above 100 kN/mm. To get a better view of less extreme variations, Figure 16 shows k_{\max}/k_{nom} when not taking into account values above 2.

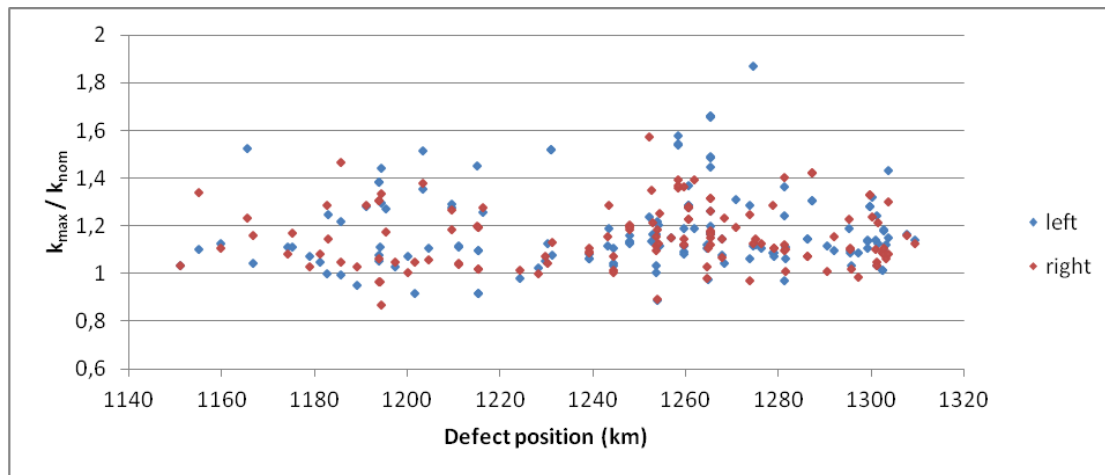


Figure 16 - Maximum track stiffness over nominal stiffness for left rail and right rail with respect to defect positions for sample 1

In Figure 16, dispersion is similar to Figure 11 for k_{\min}/k_{nom} . Some defects with a high value of k_{\max}/k_{nom} (between 1.4 and 1.8) also have a low k_{\min}/k_{nom} (below 0.6). In addition, defects that have k_{\min}/k_{nom} close to 1, but a high ratio k_{\max}/k_{nom} can be noted. In this way, the additional study of k_{\max}/k_{nom} provides a complete investigation of significant stiffness deviations around defects.

Scatters of k_{\min}/k_{nom} and k_{\max}/k_{nom} for the four other samples are presented in Appendix 9.5. It has been noticed that for sample 5 the scattering of k_{\min}/k_{nom} and k_{\max}/k_{nom} is much closer to 1. Values are not below 0.6 for k_{\min}/k_{nom} and do not exceed 1.4 for k_{\max}/k_{nom} . From the given information, it does not seem to be due to climatic conditions (temperatures). A possible explanation might be a difference in calibration (as samples 1 to 4 have been recorded in 2012 and sample 5 in November 2013).

To get to a final conclusion on the possible link between track stiffness and the occurrence of cracks, the derived ratios of k_{\min}/k_{nom} and k_{\max}/k_{nom} should be contrasted to ratios at sections where no defects have been detected.

It should be noted that the track stiffness measurements studied here have been filtered at 12 meters, according to EBER Dynamics' method, detailed in [1]. This filtering process does not allow identifying isolated hanging sleepers as the wavelength is too large. In section 5.1.3 (below), deflection with short wavelength content included has been studied in order to focus on hanging sleepers.

5.1.3 Analysis of filtered deflection deviations around detected defects

In the same way as section 5.1.2, deviations of deflection with high frequency content included are evaluated near detected defects. Deflection from database (see 3.1) has been employed and wavelengths out of the range 1-8 meters have been filtered out. As measurements have a base level of zero, the nominal value (average) is zero and thus the ratio u/u_{nom} has no meaning. Therefore, a swept standard deviation, over a moving distance of 150 meters, has been analyzed. The maximum value of this swept standard

deviation, u_{std_max} , is calculated around each defect, as well as the average (over a distance of 200 meters around the defect) of the swept standard deviation, u_{std_nom} (in the same way as for the stiffness, with the method described in section 4.1.3). The ratio u_{std_max}/u_{std_nom} is then estimated for each rail defect. Figure 17 shows the results for sample 1, Appendix 9.6 presents the obtained results for samples 2 to 5.

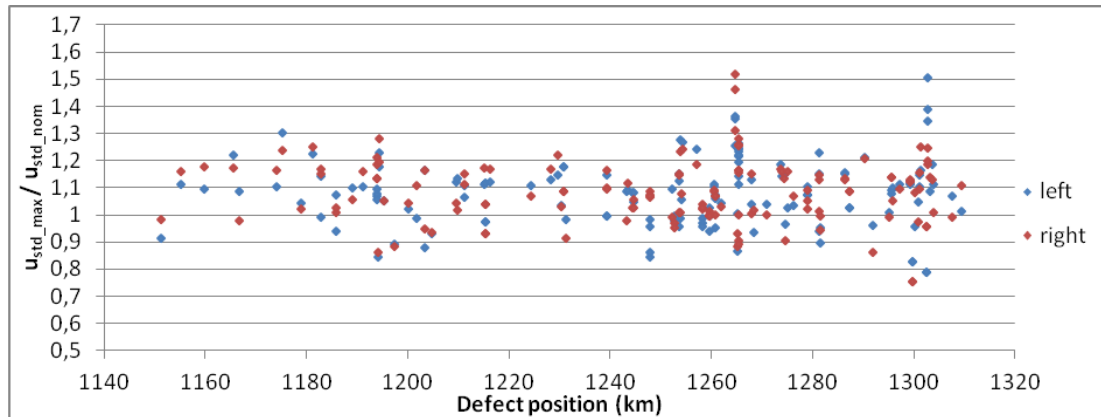


Figure 17 - Maximum swept standard deviation over nominal swept standard deviation of filtered deflection for left rail and right rail with respect to defect positions for sample 1

Values close to 1 indicate a small deflection at the studied position. The majority of the values are included between 0.8 and 1.2, but some locations show important deviations (e.g. near positions 1265 km and 1302 km). However a final conclusion on relevant correlation between deflection deviations and rail defects is not possible as long as u_{std_max}/u_{std_nom} has not been evaluated at positions where there are no defect. To do this in a statistically stringent manner is not straightforward and has not been done in the current report.

5.2 Finite elements simulations of bending moments in the vicinity of hanging sleepers

The numerical model is described in detail in the section 4.2.

5.2.1 General comments on results

For given positions of the four wheels, the finite element code ANSYS has been used to derive the deflection (or y-displacement) and the bending moment along the rail. As an example, for the case of one hanging sleeper (no stiffness at all for the spring which links the rail to the ground) and the second wheel located precisely above this sleeper, the deflection and the corresponding bending moment are depicted on the following figures (Figure 18 and Figure 19). All remaining parameters are specified for the reference case in section 4.2.

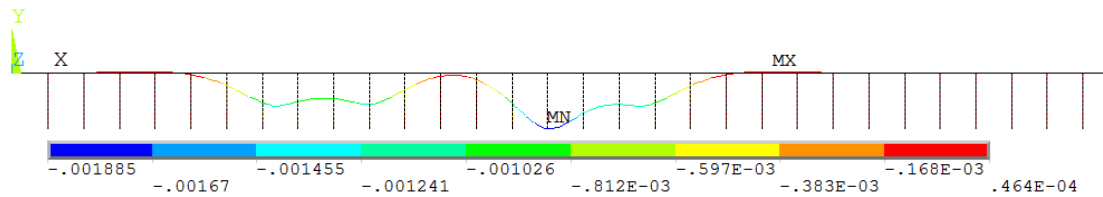


Figure 18 - Track deflection (m) corresponding to a four-wheel vehicle with one wheel positioned directly above the hanging sleeper

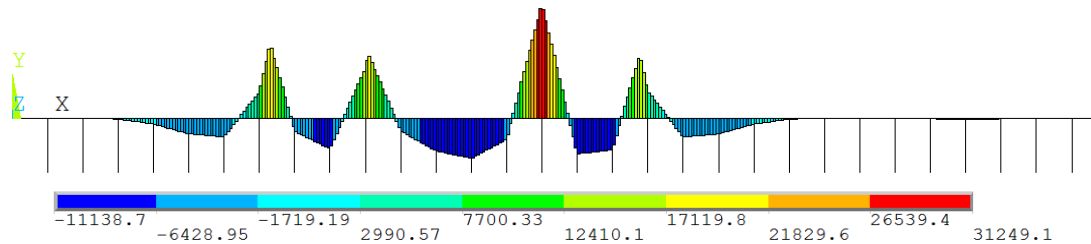


Figure 19 - Bending moment (Nm) for the same configuration as in Figure 18

A positive value for the bending moment corresponds to tension in the rail foot, whereas a negative value indicates a tensile stress in the head of the rail.

When comparing the values of deflection and bending moment obtained here with results given in [4], they are of the same order of magnitude. Simulations with the same input parameters have been run and give results very similar to [4], which supports the validity of the employed model.

What can be observed from these preliminary results is that the positive bending moment is locally increased due to the hanging sleeper at the exact position where the hanging sleeper is. However, also negative bending moments are influenced by the presence of a hanging sleeper, but this occurs in the area surrounding the hanging sleeper. One point of this study is to focus on the length of this affected zone.

5.2.2 One hanging sleeper

In the simulations one hanging sleeper is located at 9.75 m along the 20-meter rail. The stiffness of the hanging sleeper is indicated as percentage of the nominal ballast stiffness (50 MN/m). For example a reduction factor of 75% ($k=75\%$ on the graphs) means that the stiffness of the hanging sleeper is 37.5 kN ($k_{h.s.} = 0.75 * k_{nom}$). The rail bending moment and vertical displacement (deflection) are computed at each step when the four wheels travel along the rail (one wheel is represented by a 125 kN load). Maxima and minima (regarding all evaluated wheel positions) of these two parameters are evaluated. The results are presented in graphs where the distance along the track (from 5 to 15 to avoid boundary effects) is presented on the horizontal axis.

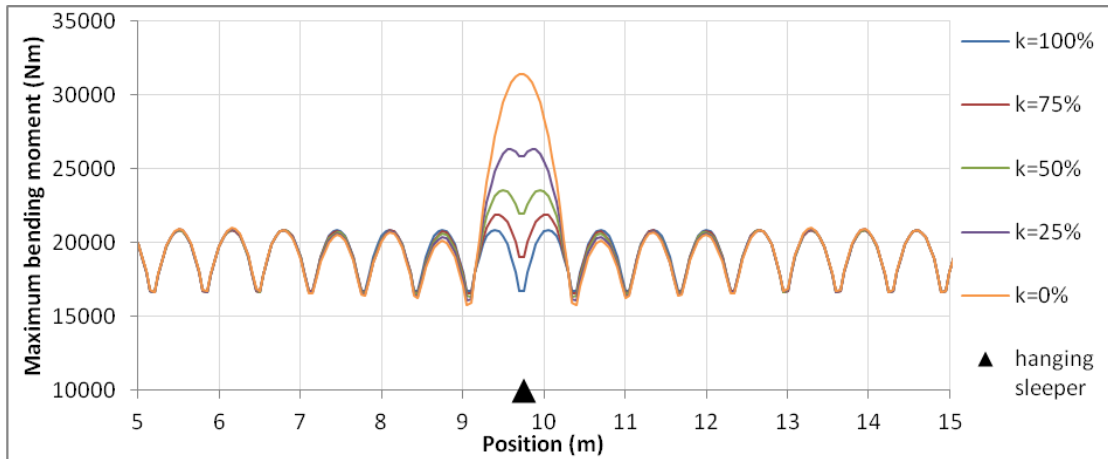


Figure 20 - Maximum bending moment, considering a hanging sleeper of stiffness 100%, 75%, 50%, 25% and 0% of the nominal track stiffness

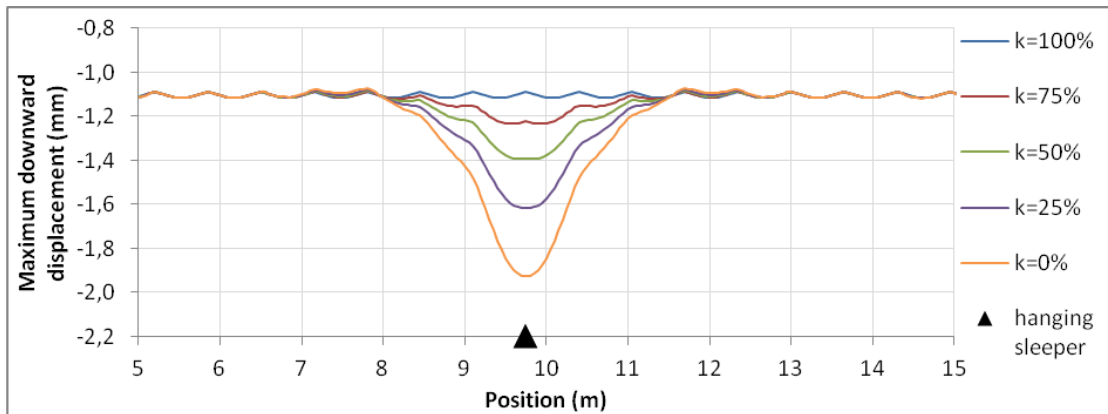


Figure 21 - Minimum displacement, considering a hanging sleeper of stiffness 100%, 75%, 50%, 25% and 0% of the nominal track stiffness

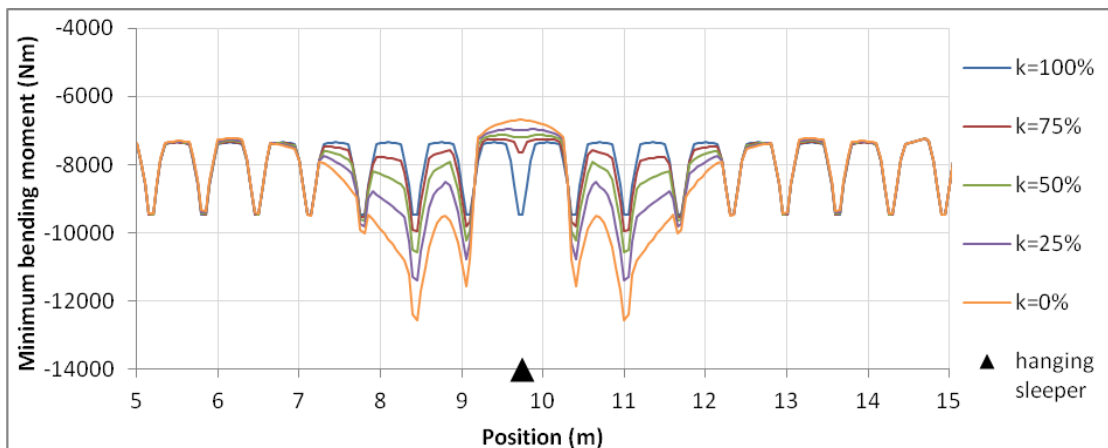


Figure 22 - Minimum bending moment, considering a hanging sleeper of stiffness 100%, 75%, 50%, 25% and 0% of the nominal track stiffness

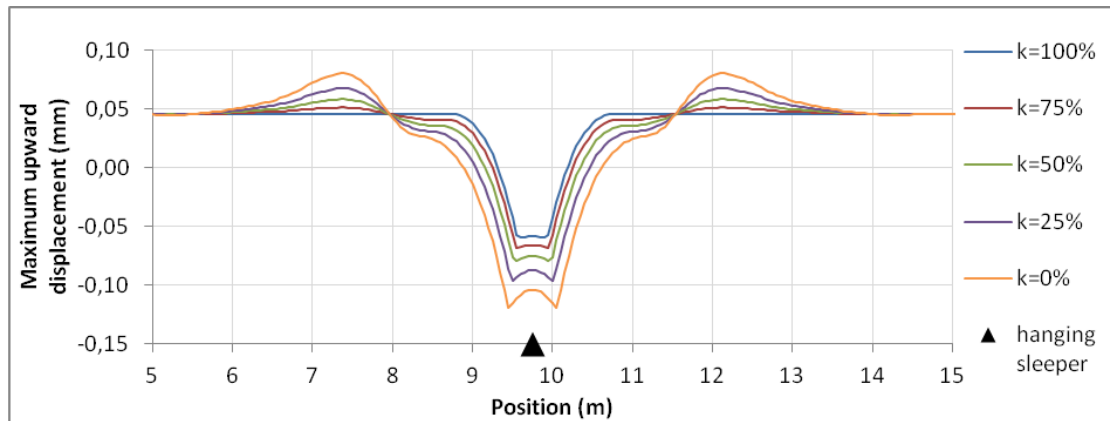


Figure 23 - Maximum displacement, considering a hanging sleeper of stiffness 100%, 75%, 50%, 25% and 0% of the nominal stiffness

First we can observe in Figure 20 and Figure 21 the rise of bending moment and deflection due to a partially or totally hanging sleeper (as defined by the stiffness reduction factor). It is possible to investigate the percentage of increase of bending moment or deflection for the different reduced stiffness as compared to the case without hanging sleeper. This has already been studied in [4].

The positive bending moment is locally increased, approximately over a length of 1 meter surrounding the hanging sleeper (50 cm on each side of the hanging sleeper), whereas the corresponding deflection is increased over a longer length of some 3.5 meters.

The minimum bending moment and the corresponding maximum displacement, as showed in Figure 22 and Figure 23, have a more complex distribution. It is seen that the length affected by the presence of a hanging sleeper is much more widespread than the affected length for the maximum bending moment. To determine this affected length it is more convenient to plot the difference in minimum bending moment for a hanging sleeper and without hanging sleeper (see Figure 24).

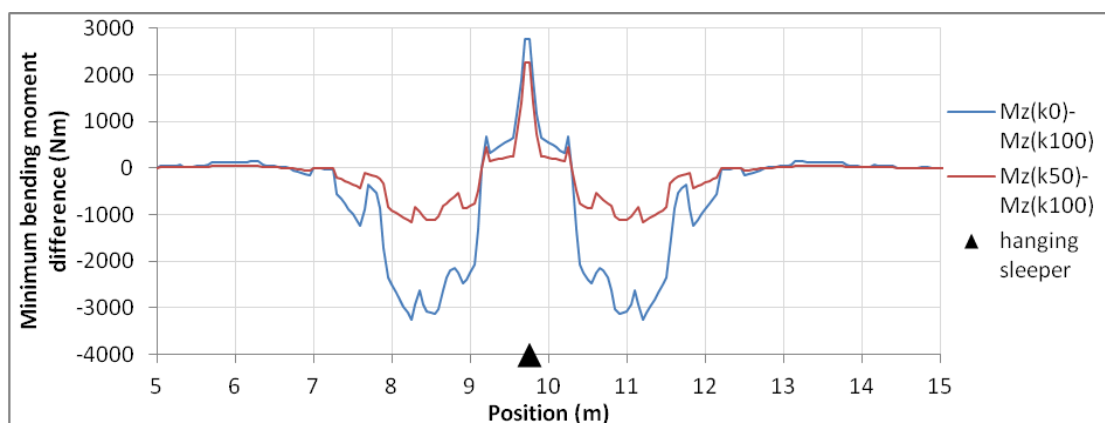


Figure 24 - Minimum bending moment difference between the case of a hanging sleeper (k=0% or k=50%) and the case without a hanging sleeper (k=100%)

A negative value of the difference means a decreased bending moment in the rail. However, as we are considering the minimum bending moment (Figure 22), the sign of the bending moment is negative and thus a decrease of its value stands for an

increase in absolute values, and a corresponding increase in the maximum stress in the cross-section.

The affected length is basically the same regardless of the stiffness reduction factor. We can estimate this length to some 5.1 meters (from 7.2 to 12.3 m). This can be interpreted as the following: the presence of a hanging sleeper increases the bending moment over a distance of some 5 meters in the studied cases. Thereby rail cracks are more likely to occur in a five-meter region surrounding a hanging sleeper.

Variation of the bending moment, i.e. top-to-top values, may also be considered. As the train moves along the track, bending moment in the rail passes from its maximum to minimum value at each location. As a consequence, the head and foot of the rail are subjected to alternating tensile and compressing stresses. This cycle promotes fatigue of the rail.

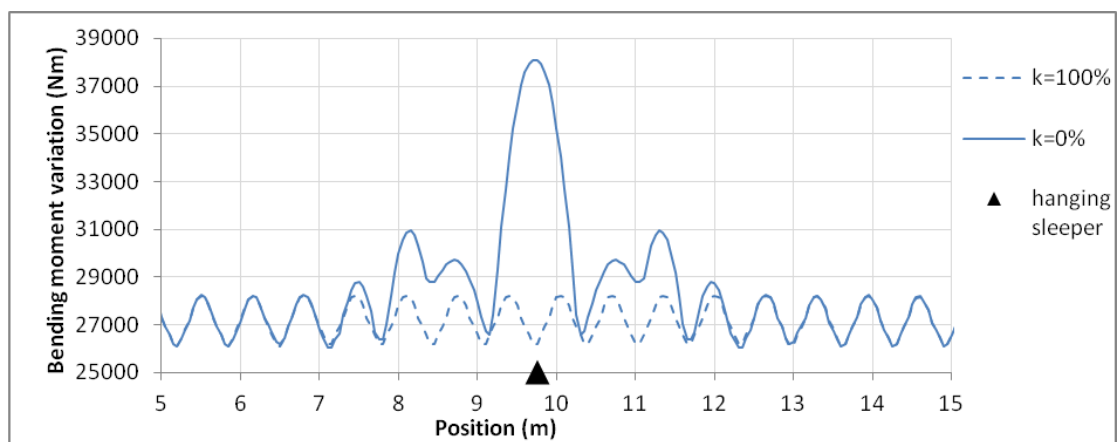


Figure 25 - Maximum variation of the bending moment (top-to-top amplitude), with a hanging sleeper (k=0%) compared to no hanging sleeper (k=100%)

In Figure 25, the length affected by the hanging sleeper is measured to some 4.7 meters (from 7.4 to 12.1 m), which is similar to the previously estimated value.

5.2.3 Several hanging sleepers

Having stated that the existence of a hanging sleeper affects the bending moment over a fixed portion of the rail, the next investigation relates whether this portion surrounding the sleeper is modified when there is more than one hanging sleeper.

Three configurations have been considered:

- 2 consecutive hanging sleepers at positions 9.75 and 10.4 m (1)
- 2 hanging sleepers separated by a normal sleeper, at positions 9.1 and 10.4 m (2)
- 3 consecutive hanging sleepers at positions 9.1, 9.75 and 10.4 m (3)

Maximum and minimum bending moments in the rail for each configuration compared to “normal” configuration (no hanging sleeper) are represented in Appendix 9.7. In Figure 26 and Figure 27 are plotted the differences between maximum or

minimum bending moments in the configuration (1), (2) and (3) ($M_{z_{\max_hs}}$ or $M_{z_{\min_hs}}$) and maximum or minimum bending moments without hanging sleeper ($M_{z_{\max_no_hs}}$ or $M_{z_{\min_no_hs}}$): $M_{z_{\max_hs}} - M_{z_{\max_no_hs}}$ or $M_{z_{\min_hs}} - M_{z_{\min_no_hs}}$

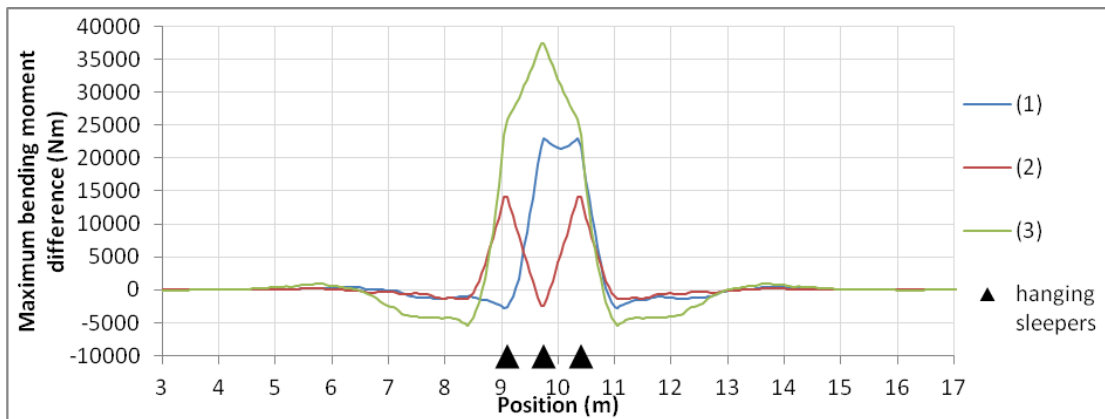


Figure 26 - Maximum bending moment difference between a configuration without a hanging sleeper and (1) two consecutive hanging sleepers ; (2) two hanging sleepers separated by a normal sleeper ; (3) three consecutive hanging sleepers

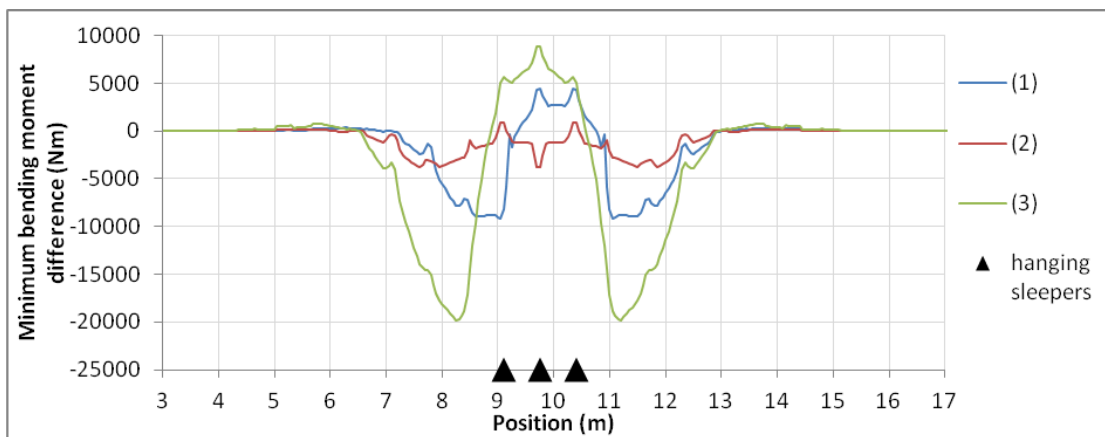


Figure 27 - Minimum bending moment difference between a configuration without hanging sleeper. (1) two consecutive hanging sleepers ; (2) two hanging sleepers separated by a normal sleeper ; (3) three consecutive hanging sleepers

Figure 28 and Figure 29 compares the distance affected by the presence of hanging sleepers, in different configurations, regarding maximum (Figure 26) or minimum (Figure 27) bending moment.

	(1)	(2)	(3)
Start – end of affected distance (m)	9.25 – 10.9	8.6 – 10.9	8.7 – 10.8
Total affected length (m)	1.65	2.3	2.1
Length to/from the first/last h.s. (m)	0.5	0.5	0.4

Figure 28 - Details on affected track length due to hanging sleepers, regarding maximum bending moment

	(1)	(2)	(3)
Start – end of affected distance (m)	7.25 – 12.9	6.6 – 12.9	6.6 – 12.9
Total affected length (m)	5.65	6.3	6.3
Length to/from the first/last h.s. (m)	2.5	2.5	2.5

Figure 29 - Details on affected track length due to hanging sleepers, regarding minimum bending moment

For the maximum bending moment (Figure 26), negative values are not accounted for when the distance is estimated (Figure 28) since it means that bending moment has been reduced.

The last row of the tables gives the affected length to the left of the first hanging sleeper, or to the right of the last hanging sleeper (these distances are the same since the model is symmetric). This distance is basically constant regardless of the chosen configuration and roughly the same as the case of one hanging sleeper. This implies that the bending moment in the rail will be increased (or decreased for negative values) at a fixed distance outside a hanging sleeper regardless of the number of hanging sleepers.

5.2.4 Variation of the input parameters

The study cases that have been presented previously have the same input. In this section input data are varied to investigate if they have an influence on the results. The investigated input parameters are the applied wheel load and the nominal track stiffness.

The load was initially set to 125 kN (corresponding to a quasi-static loading at an axle load of 25 tonnes). Here a load of 175 kN (for an axle load of 35 tonnes, which is higher than the highest regulated static axle load of 30 tonnes) and a load of 75 kN (corresponding to a static axle load of 15 tonnes) are considered. Regarding the track stiffness, it was initially fixed to 50 MN/m. In these simulations values of 30 MN/m and 70 MN/m are tested.

The maximum and minimum bending moments are computed for a model with one hanging sleeper (stiffness of 0% the nominal stiffness) and compared to a model without hanging sleeper (stiffness of 100% the nominal stiffness). Resulted graphs are presented in Appendix 9.8.

The following plots (Figure 30 and Figure 31) show the difference in minimum bending moment between a model featuring a hanging sleeper and a nominal track, for varying load and varying stiffness, respectively. We do not present the difference in maximum bending moment, as the affected length is very short, centered at the hanging sleeper.

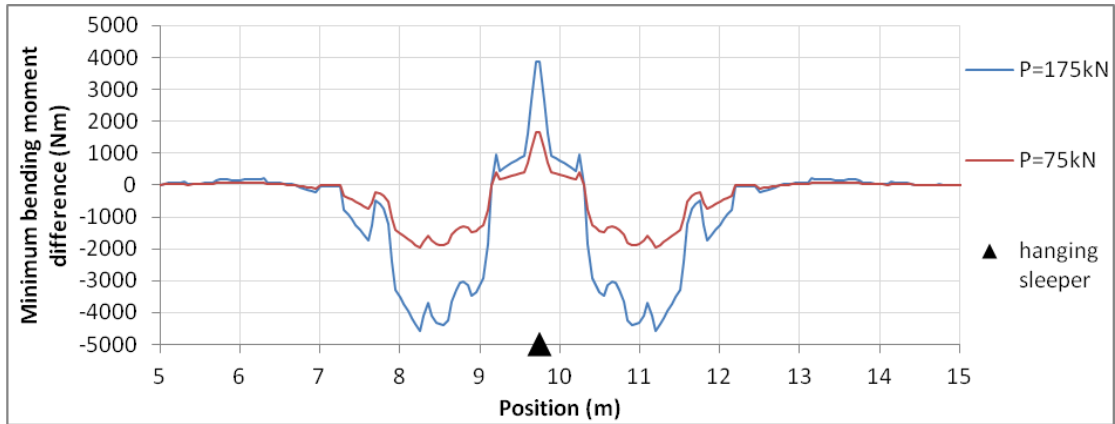


Figure 30 - Minimum bending moment differences between cases with and without a hanging sleeper, for different stiffness magnitudes

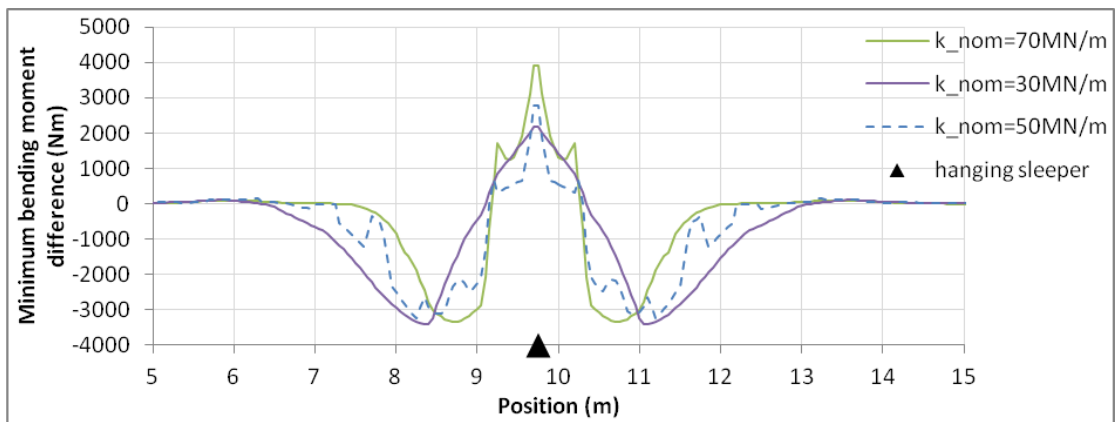


Figure 31 - Minimum bending moment differences between cases with and without a hanging sleeper, for different stiffness magnitudes

Negative values indicate an increase of the bending moment in terms of absolute values, when there is a hanging sleeper. Concerning the load parameter, Figure 30 shows clearly that the load has no influence on the length affected by the hanging sleeper. This distance is estimated to some 5.1 meters and is identical to the one estimated for a load of 125 kN presented on Figure 24. The same conclusion cannot be made regarding the nominal track stiffness. For a nominal stiffness of 70 MN/m the affected length is some 4.5 meters (from 7.5 to 12 m) whereas for a stiffness of 30 MN/m it extends to some 6.5 meters (from 6.5 to 13 m).

Nominal ballast stiffness	Total affected length	Affected length on one side
30 MN/m	6,5 m	3,25 m
50 MN/m	5,1 m	2,55 m
70 MN/m	4,5 m	2,25 m

Figure 32 - Length affected by a hanging sleeper for different track stiffness magnitudes

5.2.5 Application with real stiffness values (from measurement database)

In the previous simulations stiffness was entered as an input parameter so that the studied cases were “ideal”, in the way that only “perfect” sleepers with a constant nominal stiffness and hanging sleepers with a reduced stiffness were considered. In reality, when looking at track stiffness measurements, variations are observed, with alternatively increases and decreases of the stiffness.

With the current numerical model, it is possible to input real track stiffness values, taken from the database. However, measured track stiffness is not directly equal to the modeled stiffness. Considering the following notations:

k_i : local ballast stiffness, springs’ stiffness in the numerical model (see Figure 33),

K_i : measured track stiffness averaged over 65 cm around a sleeper,

X : ballast nominal stiffness, assuming $X = 50 \text{ MN/m}$,

Y : measured nominal track stiffness, i.e. average over the entire section,

It reads: $k_i / K_i = X / Y$ or $k_i = X / Y * K_i$

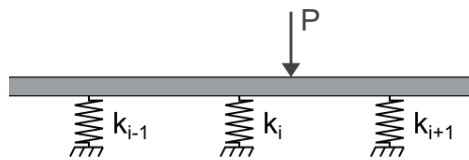


Figure 33 - Mechanical scheme of the rail, considering stiffness values from database

The defect located at 1265.433 km (ultrasonic testing database) has been chosen to illustrate this simulation. Track stiffness of the right rail in the vicinity of this defect is represented in Figure 34, on a portion of 20 meters as the modeled rail is a beam of this length.

This defect has been chosen for having a short wavelength stiffness variation compared to other defects. However it can be seen on Figure 34 that this wavelength is still large, approximately 25 meters, whereas sleepers are spaced out of 65 cm. It points out the fact that stiffness variations are roughly spread over 40 sleepers (at least) and therefore the measurements do not allow identifying one isolated hanging sleeper for instance.

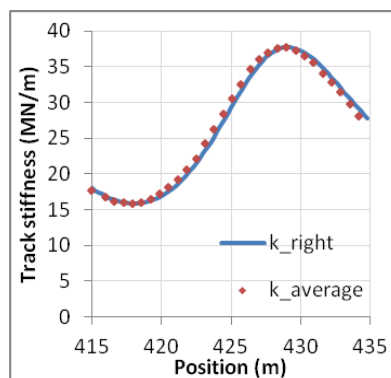


Figure 34 - Track stiffness and averaged track stiffness over 65 cm of the right rail in the vicinity of a defect located at 1265.433 km ; position x is given as 1265 (km) + x (m)

Resulting maximum bending moments are given in Figure 35. Nominal track stiffness is taken as 30 MN/m.

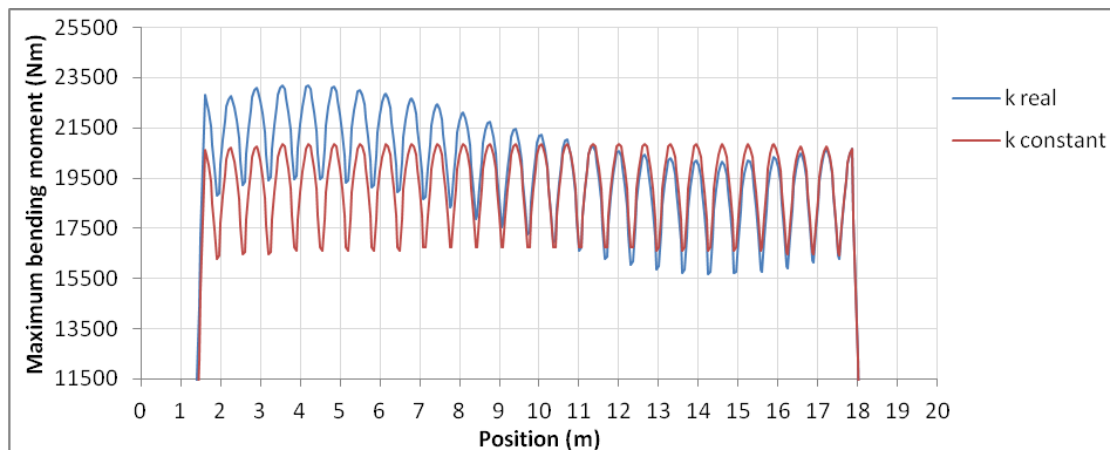


Figure 35 - Maximum bending moment around defect located at 1265.433 km, compared to a standard case with constant track stiffness (equal to nominal track stiffness of 30 MN/m)

What is observed on Figure 35 is that the bending moment is increased in the section where the track stiffness is below its nominal value.

Finally resulting bending moments here should not be taken as an example of an operational analysis as only a length of 20 meters is considered, and stiffness variations are of wavelengths larger than 25 meters (see Figure 34). Instead the example should be taken as a proof of concept on that it is possible to obtain bending moment in the rail with real stiffness values taken from measurement database. Simulations of bending moment based on measured track stiffness on longer sections could lead to interesting results.

6 Conclusion

In the first part, the correlation between track characteristics measurement and defect positions has been investigated. It seems that there is no straightforward correlation. Indeed, for a given defect, some of the relevant parameters (longitudinal level, deflection, track stiffness...) can present notable deviations while others do not. It is also applicable for a given parameter: some defects are positioned at sections where there are significant variations while others do not.

An in-depth investigation has been realized for track stiffness and deflection around recorded defects. Measures such as ratios between minimal track stiffness over nominal track stiffness, or maximal swept standard deviation of deflection with short wavelength content over its nominal value have been analysed. The analysis of deviations at locations of detected defects shows correlations for some, but not all defects. This conclusion was expected as track stiffness variations are not the only reason of crack formation and crack growth. However, locally decreased track stiffness should increase the risk of crack formation. If there is such an increase that is statistically significant was not possible to establish within the current study.

In the second part of the work, the influence of hanging sleepers, which can be seen as short wavelength stiffness variations, on the bending moment along the rail has been studied. It has been shown that a specific distance where bending moment is increased in the surrounding of hanging sleepers can be defined. This distance is representative of the length for potentially increased risk of rail crack growth. These results should also be considered in light of the fact that in most cases, it is the unlucky combination of hanging sleepers in regions with proneness to crack formation (e.g. shallow curves where headcheck cracks may form) that promotes fast crack growth and subsequent failure. Inspections should thus investigate for head cracks in an interval spanning of some 4 sleepers in both directions from a detected hanging sleeper.

7 Recommendations

The purpose of this work is to be able to predict defect occurrence from measurement of track characteristics. At this stage, the realized work can be improved with the following actions:

- Improve accuracy of position in crack detection: there is an uncertainty of 20 meters of the position between the two databases. Deviation ratios such as k_{\min}/k_{nom} or u_{\min}/u_{std} (see 5.1.2 and 5.1.3) could be refined and then become more relevant if this distance was decreased.
- Check cause(s) of high stiffness. In part 5.1.2, stiffness variations plotted around defects with a notable low ratio k_{\min}/k_{nom} in several cases revealed large stiffness peaks. Going deeper in the study of these extreme values would enable to determine if they are significant for defect formation or not.
- Compute nominal values of ratios evaluated in sections 5.1.2 and 5.1.3 by establishing average values of these ratios at positions where there are no defects. This would enable a comparison of ratios derived in this report and the establishment of limit values. However, as stated above, to establish such "base values" in a statistically stringent manner is not straightforward. Since the values vary significantly along the track the definition of a "nominal" value is not obvious.
- Evaluate from database measurements the rail in which defects have been detected, in order to clarify results of 5.1.2 and 5.1.3.
- Determine a method to get raw stiffness amplitudes (not filtered at large wavelengths) to input them in finite elements simulations, in order to obtain the rail bending moment.

8 References

- [1] Berggren, E. (2013): *Track stiffness/deflection and track degradation at the Iron-ore in Sweden*, Falun, Sweden.
- [2] International Union of Railways (2002): *UIC Code – Rail defects*, Paris, France.
- [3] INNOTRACK (2010): *Concluding Technical Report*, Gothenburg, Sweden.
- [4] Cyrillus, C., Grundberg, J. and Korneliusson, M. (2007): *Modellering av spårstruktur – En undersökning av hur olika modeller för underlagsstyvhet påverkar predikterade böjspänningar och utböjning av en tågräl*, Chalmers Tekniska Högskola, Gothenburg, Sweden.
- [5] Nielsen, J., Kabo, E. and Ekberg, A. (2009): *Alarm limits for wheel-rail impact loads – part 1: rail bending moments generated by wheel flats*, Chalmers University of Technology, Gothenburg, Sweden.
- [6] Nielsen, J., Kabo, E. and Ekberg, A. (2009): *Alarm limits for wheel-rail impact loads – part 2: analysis of crack growth and fracture*, Chalmers University of Technology, Gothenburg, Sweden.
- [7] Kabo, E. and Ekberg, A. (2004): *Fatigue of railway wheels and rails under rolling contact and thermal loading – an overview*, Chalmers Tekniska Högskola, Gothenburg, Sweden.

9 Appendices

9.1 MATLAB code for analysis of track characteristics at detected defects

```
close all; clc; clear all;

%% Input parameter %%
defect_position=1194.238; % Position of the defect studied (km)
sample=3; % Studied sample (1 for D(1), 2 for
           % D(2), ...5 for D(5))
data1=9; % Analyzed parameter
          % Longitudinal level left side = 3
          % Mean track deflection left side = 7
          % Mean track stiffness left side = 9
          % Track deflection short wavelength left
          % side = 11
data2=data1+1; % Same than data1 for the right rail
speed_limit=10; % Speed limit of track recording (km/h)
L_around=0.2; % Length around the defect for plotting
              % (km)
delta=0.0005; % Tolerance of the interval (km)

%% Loading data file for the choosen defect %%
if (defect_position>=1150 & defect_position<1170 )
    load('deflection_data_118_1160.mat');
elseif (defect_position>=1170 & defect_position<1190 )
    load('deflection_data_118_1180.mat');
elseif (defect_position>=1190 & defect_position<1210 )
    load('deflection_data_118_1200.mat');
elseif (defect_position>=1210 & defect_position<1230 )
    load('deflection_data_118_1220.mat');
elseif (defect_position>=1230 & defect_position<1250 )
    load('deflection_data_118_1240.mat');
elseif (defect_position>=1250 & defect_position<1270 )
    load('deflection_data_118_1260.mat');
elseif (defect_position>=1270 & defect_position<1290 )
    load('deflection_data_118_1280.mat');
elseif (defect_position>=1290 & defect_position<1310 )
    load('deflection_data_118_1300.mat');
end;

%% Initialization of indexes %%
num=0;
num_inf=0;
num_sup=0;
i=0;
L=length(D(sample).m_temp); % Size of matrix of positions along
                             % the track for choosen sample

%% Determination of the indexes used to plot analyzed parameter
around the choosen defect %%

for i=1:1:L
    % Smaller index of the area where the studied parameter will
    % plotted
    if D(sample).m_temp(i,1)>(defect_position-L_around-delta) & ...
```

```

        D(sample).m_temp(i,1)<(defect_position-L_around+delta)
        num_inf=i;
    end

% Index of the position of the defect
    if D(sample).m_temp(i,1)>(defect_position-delta)& ...
        D(sample).m_temp(i,1)<(defect_position+delta)
        num=i;
    end

% Bigger index of the area where the studied parameter will be
% plotted
    if D(sample).m_temp(i,1)>(defect_position+L_around-delta)& ...
        D(sample).m_temp(i,1)<(defect_position+L_around+delta)
        num_sup=i;
    end
end;

%% Low velocity preprocessing %%
% Calculation of average of studied parameter that will be used to
% replace value where velocity is lower than "speed_limit"

moyenne_1=mean((D(sample).data(num_inf:num_sup,data1)));
moyenne_2=mean((D(sample).data(num_inf:num_sup,data2)));

% For the choosen values around the defects, if recording velocity is
% too low, value of parameter is changing with the avergae value of
% the studied parameter

for i=num_inf:1:num_sup
    if D(sample).data(i,6)<speed_limit
        A(i,1)=moyenne_1;
        B(i,1)=moyenne_2;
    else A(i,1)=(D(sample).data(i,data1));
        B(i,1)=(D(sample).data(i,data2));
    end
end;

%% Plot %%
% Plotting studied parameter for both rails according to the position
% along the track
fig1=figure;
plot(D(sample).m_temp(num_inf:num_sup,1),A(num_inf:num_sup,1));
hold on
plot(D(sample).m_temp(num_inf:num_sup,1),B(num_inf:num_sup,1),'red');
%% Legends %%
% Legend of the figure
legend('left','right');
xlabel('position [km]');

% Label according to the studied parameter
if data1==3 | data1==4
    ylabel('longitudinal level [mm]');
elseif data1==7 | data1==8
    ylabel('mean track deflection [mm]');
elseif data1==9 | data1==10
    ylabel('mean track stiffness [kN/mm]');
elseif data1==11 | data1==12
    ylabel('track deflection with short wavelength [mm]');
elseif data1==13 | data1==14

```

```
        ylabel('longitudinal level with waveband 1-25m [mm]');
elseif data1==15 | data1==16
        ylabel('longitudinal level with waveband 3-9m [mm]');
elseif data1==17 | data1==18
        ylabel('longitudinal level with waveband 1-4m [mm]');
end ;

%%%%%%%%%%%%%%%%%%%%%%%%%%%%%%%%%%%%%%%%%%%%%%%%%%%%%%%%%%%%%%%%%%%%%%%%%
```

9.2 MATLAB code for local track stiffness deviations

```
close all; clc; clear all;

%% Input parameter %%
sample=1;           % 1 for D(1), 2 for D(2), ...
L_around=0.020;    % Length around the defect for calculating
                  % minimal stiffness(km)
L_average=0.100;   % Length around the defect where the nominal
                  % stiffness is calculated (km)
delta=0.0005;      % Tolerance of the interval (km)

%% Loading Measurement of ultrasonic testing for section 118 %%
[num, txt, tab] = xlsread('Ultrasonic measurements_118.xlsx'); %

%% Loading data file for the choosen defect %%
nb_defect=length(num(:,1)); % Number of defects

for defect=1:1:nb_defect

% Storing defect position for all defects
    position_defect(defect,1)=num(defect,13);
% loading file
    if (position_defect(defect)>=1150 & position_defect(defect)<1170)
        load('deflection_data_118_1160.mat');
        file_loaded(defect,1)=1160;
    elseif (position_defect(defect)>=1170 &
position_defect(defect)<1190)
        load('deflection_data_118_1180.mat');
        file_loaded(defect,1)=1180;
    elseif (position_defect(defect)>=1190 &
position_defect(defect)<1210)
        load('deflection_data_118_1200.mat');
        file_loaded(defect,1)=1200;
    elseif (position_defect(defect)>=1210 &
position_defect(defect)<1230)
        load('deflection_data_118_1220.mat');
        file_loaded(defect,1)=1220;
    elseif (position_defect(defect)>=1230 &
position_defect(defect)<1250)
        load('deflection_data_118_1240.mat');
        file_loaded(defect,1)=1240;
    elseif (position_defect(defect)>=1250 &
position_defect(defect)<1270)
        load('deflection_data_118_1260.mat');
        file_loaded(defect,1)=1260;
    elseif (position_defect(defect)>=1270 &
position_defect(defect)<1290)
        load('deflection_data_118_1280.mat');
        file_loaded(defect,1)=1280;
    elseif (position_defect(defect)>=1290 &
position_defect(defect)<1310)
        load('deflection_data_118_1300.mat');
        file_loaded(defect,1)=1300;
    end

%% Initialization of indexes %%
    inf_average=0;
    sup_average=0;
    inf_around=0;
```

```

sup_around=0;
L=length(D(sample).m_temp); % Size of matrix of positions
                             % along the track for choosen
                             % sample

%% Determination of the indexes used to calculate minimum and nominal
stiffness on L_around and L_average %%

    for i=1:L
        if D(sample).m_temp(i,1)>(position_defect(defect)-L_average-
delta)& D(sample).m_temp(i,1)<(position_defect(defect)-
L_average+delta)
            inf_average=i;
        elseif
D(sample).m_temp(i,1)>(position_defect(defect)+L_average-delta)&
D(sample).m_temp(i,1)<(position_defect(defect)+L_average+delta)
            sup_average=i;
        elseif D(sample).m_temp(i,1)>(position_defect(defect)-
L_around-delta)& D(sample).m_temp(i,1)<(position_defect(defect)-
L_around+delta)
            inf_around=i;
        elseif
D(sample).m_temp(i,1)>(position_defect(defect)+L_around-delta)&
D(sample).m_temp(i,1)<(position_defect(defect)+L_around+delta)
            sup_around=i;
        end
    end

%% Storing minimum stiffness and its position for both rails %%
[k_min_left(defect,1)
ind_kmin_left]=min(D(sample).data(inf_around:sup_around,9));
[k_min_right(defect,1)
ind_kmin_right]=min(D(sample).data(inf_around:sup_around,10));

position_kmin_left(defect,1)=D(sample).m_temp(ind_kmin_left+inf_around,1);
position_kmin_right(defect,1)=D(sample).m_temp(ind_kmin_right+inf_around,1);

%% Storing maximum stiffness and its position for both rails %%
[k_max_left(defect,1)
ind_kmax_left]=max(D(sample).data(inf_around:sup_around,9));
[k_max_right(defect,1)
ind_kmax_right]=max(D(sample).data(inf_around:sup_around,10));

position_kmax_left(defect,1)=D(sample).m_temp(ind_kmax_left+inf_around,1);
position_kmax_right(defect,1)=D(sample).m_temp(ind_kmax_right+inf_around,1);

%% Storing nominal stiffness for both rails %%
k_nom_left(defect,1)=mean(D(sample).data(inf_average:sup_average,9));
k_nom_right(defect,1)=mean(D(sample).data(inf_average:sup_average,10));

%% Computing ratio k_min / k_nom for both rails %%
ratio_kmin_left(defect,1)=k_min_left(defect,1)./k_nom_left(defect,1);
ratio_kmin_right(defect,1)=k_min_right(defect,1)./k_nom_right(defect,1);

```

```

%% Computing ratio k_max / k_nom for both rails %%
ratio_kmax_left(defect,1)=k_max_left(defect,1)./k_nom_left(defect,1);
ratio_kmax_right(defect,1)=k_max_right(defect,1)./k_nom_right(defect,
1);

end;

%% Writing the results in Excel file %%

filename = 'Results_k_min_kmax_knom.xlsx';
Column_title={ 'k_min left' ...
'k_max left' ...
'k_nom left' ...
'k_min/k_nom left' ...
'k_max/k_nom left' ...
'k_min right' ...
'k_max right' ...
'k_nom right' ...
'k_min/k_nom right' ...
'k_max/k_nom right' ...
'defect position' ...
'position k_min left' ...
'position k_max left' ...
'position k_min right'...
'position k_max right'};
xlswrite(filename, Column_title)
xlswrite(filename,k_min_left(:,1),1,'A2');
xlswrite(filename,k_max_left(:,1),1,'B2');
xlswrite(filename,k_nom_left(:,1),1,'C2');
xlswrite(filename,ratio_kmin_left(:,1),1,'D2');
xlswrite(filename,ratio_kmax_left(:,1),1,'E2');
xlswrite(filename,k_min_right(:,1),1,'F2');
xlswrite(filename,k_max_right(:,1),1,'G2');
xlswrite(filename,k_nom_right(:,1),1,'H2');
xlswrite(filename,ratio_kmin_right(:,1),1,'I2');
xlswrite(filename,ratio_kmax_right(:,1),1,'J2');
xlswrite(filename,position_defect(:,1),1,'K2');
xlswrite(filename,position_kmin_left(:,1),1,'L2');
xlswrite(filename,position_kmax_left(:,1),1,'M2');
xlswrite(filename,position_kmin_right(:,1),1,'N2');
xlswrite(filename,position_kmax_right(:,1),1,'O2');

%%%%%%%%%%%%%%%%%%%%%%%%%%%%%%%%%%%%%%%%%%%%%%%%%%%%%%%%%%%%%%%%%%%%%%%%

```

9.3 ANSYS command file for estimating bending moments in a rail with hanging sleepers

```

/BATCH
WPSTYLE,,,,,,,,,0

/PREP7                ! Open the Preprocessor module

!!!!!!!!!!!!!!!!!!!! variables !!!!!!!!!!!!!!!!!!!!!

reduc=0                ! Reducing factor of stiffness for the hanging sleeper (%)
k_norm=30E6            ! Stiffness for "normal" sleepers (N/m)
load=250000/2         ! Load per wheel=axial load/2 (N)

!!!!!!!!!!!!!!!!!!!! Element types !!!!!!!!!!!!!!!!!!!!!

ET,1,BEAM188          ! Element type 1 = Beam188
ET,2,COMBIN14         ! Element type 2 = Combin14 (spring-damper)
ET,3,COMBIN14         ! Element type 3 = Combin14 (spring-damper)

!!!!!!!!!!!!!!!!!!!! Real constants !!!!!!!!!!!!!!!!!!!!!

K_hang=reduc*k_norm/100 ! Stiffness for the hanging sleeper
R,2,k_norm, , , , ,    ! Stiffness for element 2 -> Normal sleepers
R,3,k_hang, , , , ,    ! Stiffness for element 3 -> Hanging sleeper

!!!!!!!!!!!!!!!!!!!! Material properties !!!!!!!!!!!!!!!!!!!!!

MPTEMP,,,,,,,,
MPTEMP,1,0
MPDATA,EX,1,,210E9     ! Young modulus
MPDATA,PRXY,1,,0.3     ! Poisson coefficient
MPDATA,DENS,1,,7862    ! Density

!!!!!!!!!!!!!!!!!!!! Beam section !!!!!!!!!!!!!!!!!!!!!

SECTYPE, 1, BEAM, ASEC, , 0
SECOFFSET, CENT
SECDATA,76.70E-4,512.3E-8,0,3038.3E-8,0,3.05E-5,0,0,0,0,150E-3,172E-3

!!!!!!!!!!!!!!!!!!!! Nodes !!!!!!!!!!!!!!!!!!!!!

xpos1=0                ! xpos initialization
*DO,I,1,401            ! For I = 1 to 401 (there will be 401 nodes)
N,I,xpos1,0,0          ! Create a node I, at location dxpos,0,0
xpos1=xpos1+0.05      ! xpos is the incremented x position
*ENDDO

xpos2=0.65            ! Nodes for the bottom end of springs
*DO,I,1001,1030
N,I,xpos2,-1,0
xpos2=xpos2+0.65
*ENDDO

!!!!!!!!!!!!!!!!!!!! Elements !!!!!!!!!!!!!!!!!!!!!

TYPE, 1                ! Meshing with element type 1 (beam)
MAT, 1
REAL, ,
ESYS, 0
SECNUM, 1
TSHAP,LINE

E,1,2
*REPEAT,400,1,1

TYPE, 2                ! Meshing with element type 2 (spring)
MAT, 1
REAL, 2
ESYS, 0
SECNUM, ,
TSHAP,LINE

E,14,1001              ! Meshing the springs for "normal" sleepers
*REPEAT,14,13,1
E,209,1016
*REPEAT,15,13,1

```

```

TYPE, 3          ! Meshing with element type 3 (spring)
MAT, 1
REAL, 3
ESYS, 0
SECNUM, ,
TSHAP, LINE
E, 196, 1015     ! Meshing the spring for the hanging sleeper

!!!!!!!!!!!!!!!!!!!! Boundary conditions !!!!!!!!!!!!!!!!!!!!!

D, 1, UX, 0      ! BC for the first node of the rail
D, 1, UY, 0
D, 1, UZ, 0
D, 1, ROTX, 0
D, 1, ROTY, 0

D, 401, UY, 0    ! BC for the last node of the rail
D, 401, UZ, 0

D, 1001, ALL, 0  ! BC for springs' base
*REPEAT, 30, 1, 0, 0

FINISH          ! Close the Preprocessor module

!!!!!!!!!!!!!!!!!!!! Loop to vary the load positions !!!!!!!!!!!!!!!!!!!!!

Imin=170         ! First position of the 1st wheel
Imax=358         ! Last position of the 1st wheel

*DIM, deflect, ARRAY, 401, Imax-Imin+1 ! Array for saving UY results
*DIM, bend_mom, ARRAY, 401, Imax-Imin+1 ! Array for saving MZ results

*DO, I, Imin, Imax

!!!!!!!!!!!!!!!!!!!! Loads !!!!!!!!!!!!!!!!!!!!!

/PREP7          ! Open the Preprocessor module
FDELE, 2, FY, 400, 1 ! Delete forces FY for all nodes

F, I, FY, -load   ! Force for wheel 1
F, I-36, FY, -load ! Force for wheel 2
F, I-100, FY, -load ! Force for wheel 3
F, I-136, FY, -load ! Force for wheel 4

FINISH          ! Close the Preprocessor module

!!!!!!!!!!!!!!!!!!!! Solving !!!!!!!!!!!!!!!!!!!!!

/SOLU           ! Open the Solution module
SOLVE
FINISH          ! Close the solution module

!!!!!!!!!!!!!!!!!!!! Post processing !!!!!!!!!!!!!!!!!!!!!

/POST1          ! Open Postprocessor module
*VGET, deflect(1, I-Imin+1), NODE, ALL, U, Y ! Get the deflection at each node

ETABLE, MZ, SMISC, 3 ! Create table for bending moment

*DO, J, 1, 400   ! Loop for getting the bending moment at each node
*GET, bend_mom(J, I-Imin+1), ETAB, 1, ELEM, J
*ENDDO
*GET, bend_mom(401, I-Imin+1), ETAB, 1, ELEM, 400 ! Bending moment for the last element

FINISH          ! Close Postprocessor module
*ENDDO          ! End of the loop varying the load positions

!!!!!!!!!!!!!!!!!!!! Writing the results !!!!!!!!!!!!!!!!!!!!!

*CFOPEN, 'Resu_UY', 'xls', ' '
*DO, I, 0, 170, 10
*VWRITE, deflect(1, I+1), deflect(1, I+2), deflect(1, I+3), deflect(1, I+4), deflect(1, I+5), def
lect(1, I+6), deflect(1, I+7), deflect(1, I+8), deflect(1, I+9), deflect(1, I+10)
(E30.6, E30.6, E30.6, E30.6, E30.6, E30.6, E30.6, E30.6, E30.6, E30.6)
*VWRITE, ' '
(A10)

```

```

*ENDDO
*vWRITE,deflect(1,181),deflect(1,182),deflect(1,183),deflect(1,184),deflect(1,185),def
lect(1,186),deflect(1,187),deflect(1,188),deflect(1,189)
(E30.6,E30.6,E30.6,E30.6,E30.6,E30.6,E30.6,E30.6,E30.6)
*CFCLOS

*CFOPEN,'Resu_MZ','xls',' '
*DO,I,0,170,10
*vWRITE,bend_mom(1,I+1),bend_mom(1,I+2),bend_mom(1,I+3),bend_mom(1,I+4),bend_mom(1,I+5
),bend_mom(1,I+6),bend_mom(1,I+7),bend_mom(1,I+8),bend_mom(1,I+9),bend_mom(1,I+10)
(E30.6,E30.6,E30.6,E30.6,E30.6,E30.6,E30.6,E30.6,E30.6,E30.6)
*vWRITE,' '
(A10)
*ENDDO
*vWRITE,bend_mom(1,181),bend_mom(1,182),bend_mom(1,183),bend_mom(1,184),bend_mom(1,185
),bend_mom(1,186),bend_mom(1,187),bend_mom(1,188),bend_mom(1,189)
(E30.6,E30.6,E30.6,E30.6,E30.6,E30.6,E30.6,E30.6,E30.6)
*CFCLOS

```

! If considering real stiffness values, first part of the code is changed with the following:

```

/PREP7 ! Open the Preprocessor module

!!!!!!!!!!!!!!!!!!!! Variables !!!!!!!!!!!!!!!!!!!!!

load=250000/2 ! Load per wheel=axial load/2 (N)

k_tra_n=30E6 ! Nominal track stiffness - average on the section (N/m)
k_bal_n=50E6 ! Nominal ballast stiffness (N/m)

*DIM,k_track,ARRAY,30 ! Creation of an array for track stiffness averaged around each
sleeper
k_track(1,1)=29.2E6 ! Measured track stiffness averaged around the sleeper 1 to 30
(N/m)
k_track(2,1)=32.6E6
k_track(3,1)=35.9E6
k_track(4,1)=39.0E6
k_track(5,1)=42.4E6
k_track(6,1)=46.0E6
k_track(7,1)=50.0E6
k_track(8,1)=55.2E6
k_track(9,1)=59.9E6
k_track(10,1)=65.2E6
k_track(11,1)=70.8E6
k_track(12,1)=76.8E6
k_track(13,1)=84.2E6
k_track(14,1)=90.2E6
k_track(15,1)=95.8E6
k_track(16,1)=100.5E6
k_track(17,1)=103.9E6
k_track(18,1)=105.7E6
k_track(19,1)=105.3E6
k_track(20,1)=102.8E6
k_track(21,1)=98.8E6
k_track(22,1)=93.4E6
k_track(23,1)=85.9E6
k_track(24,1)=79.3E6
k_track(25,1)=72.8E6
k_track(26,1)=66.7E6
k_track(27,1)=61.2E6
k_track(28,1)=55.5E6
k_track(29,1)=51.5E6
k_track(30,1)=47.8E6

*DIM,k_local,ARRAY,30 ! Creation of an array for local ballast stiffness at each
sleeper
*DO,I,1,30
k_local(I,1)=k_bal_n*k_track(I,1)/k_tra_n ! Calculate local ballast stiffness at
each sleeper
*ENDDO

!!!!!!!!!!!!!!!!!!!! Element types !!!!!!!!!!!!!!!!!!!!!

ET,1,BEAM188 ! Element type 1 = Beam188
ET,2,COMBIN14 ! Element type 2 to 31 = Combin14 (spring-damper)
*REPEAT,30,1

!!!!!!!!!!!!!!!!!!!! Real constants !!!!!!!!!!!!!!!!!!!!!

*DO,I,2,31
R,I,k_local(I-1,1), , , , , ! Stiffness for element I
*ENDDO

```

```

!!!!!!!!!!!!!!!!!!!! Material properties !!!!!!!!!!!!!!!!!!!!!

MPTEMP,,,,,,,,
MPTEMP,1,0
MPDATA,EX,1,,210E9      ! Young modulus
MPDATA,PRXY,1,,0.3     ! Poisson coefficient
MPDATA,DENS,1,,7862    ! Density

!!!!!!!!!!!!!!!!!!!! Beam section !!!!!!!!!!!!!!!!!!!!!

SECTYPE, 1, BEAM, ASEC, , 0
SECOFFSET, CENT
SECDATA,76.70E-4,512.3E-8,0,3038.3E-8,0,3.05E-5,0,0,0,0,150E-3,172E-3

!!!!!!!!!!!!!!!!!!!! Nodes !!!!!!!!!!!!!!!!!!!!!

xpos1=0                ! xpos initialization
*DO,I,1,401            ! For I = 1 to 401 (there will be 401 nodes)
N,I,xpos1,0,0         ! Create a node I, at location dxpos,0,0
xpos1=xpos1+0.05     ! xpos is the incremented x position
*ENDDO
xpos2=0.65
*DO,I,1001,1030
N,I,xpos2,-1,0
xpos2=xpos2+0.65
*ENDDO

!!!!!!!!!!!!!!!!!!!! Elements !!!!!!!!!!!!!!!!!!!!!

TYPE, 1                ! Meshing with element type 1 (beam)
MAT, 1
REAL, ,
ESYS, 0
SECNUM, 1
TSHAP,LINE
E,1,2
*REPEAT,400,1,1

!TYPE, 2              ! Meshing with element type 2 (spring)
!MAT, 1
!REAL, 2
!ESYS, 0
!SECNUM, ,
!TSHAP,LINE
!E,14,1001           ! Meshing the springs for "normal" sleepers
!*REPEAT,14,13,1
!E,209,1016
!*REPEAT,15,13,1

!TYPE, 3              ! Meshing with element type 3 (spring)
!MAT, 1
!REAL, 3
!ESYS, 0
!SECNUM, ,
!TSHAP,LINE
!E,196,1015         ! Meshing the spring for the hanging sleeper

*DO,I,2,31            ! Meshing with element type I (spring)
TYPE, I
MAT, 1
REAL, I
ESYS, 0
SECNUM, ,
TSHAP,LINE
E,1+13*(I-1),1000+(I-1)
*ENDDO

!!!!!!!!!!!!!!!!!!!! Boundary conditions !!!!!!!!!!!!!!!!!!!!!

D, 1, UX, 0          ! BC for the first node of the rail
D, 1, UY, 0
D, 1, UZ, 0
D, 1, ROTX, 0
D, 1, ROTY, 0
D, 401, UY, 0        ! BC for the last node of the rail
D, 401, UZ, 0
D, 1001, ALL, 0     ! BC for springs'base
*REPEAT,30,1,0,0

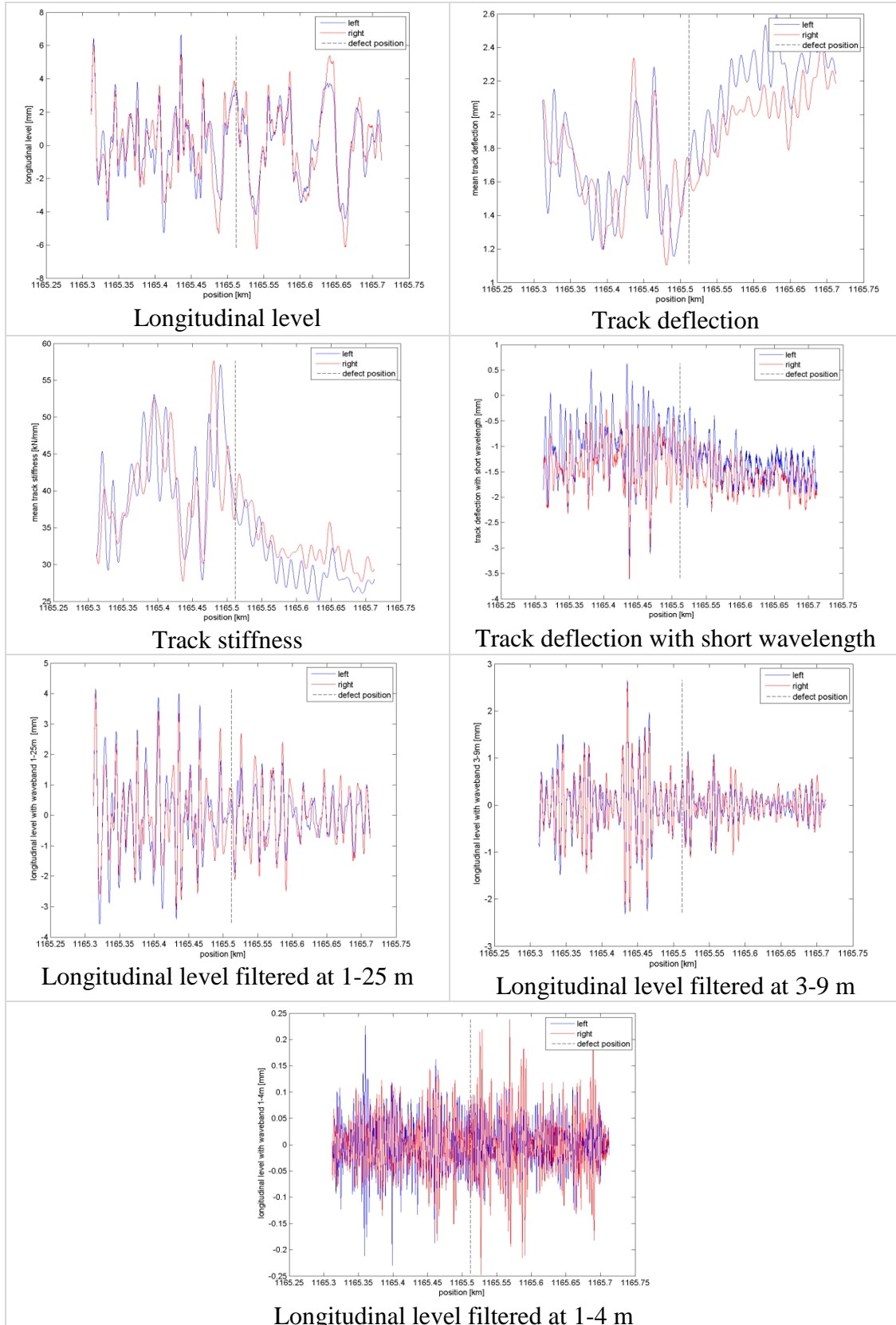
FINISH                ! Close the Preprocessor module

! Continue with the previous code

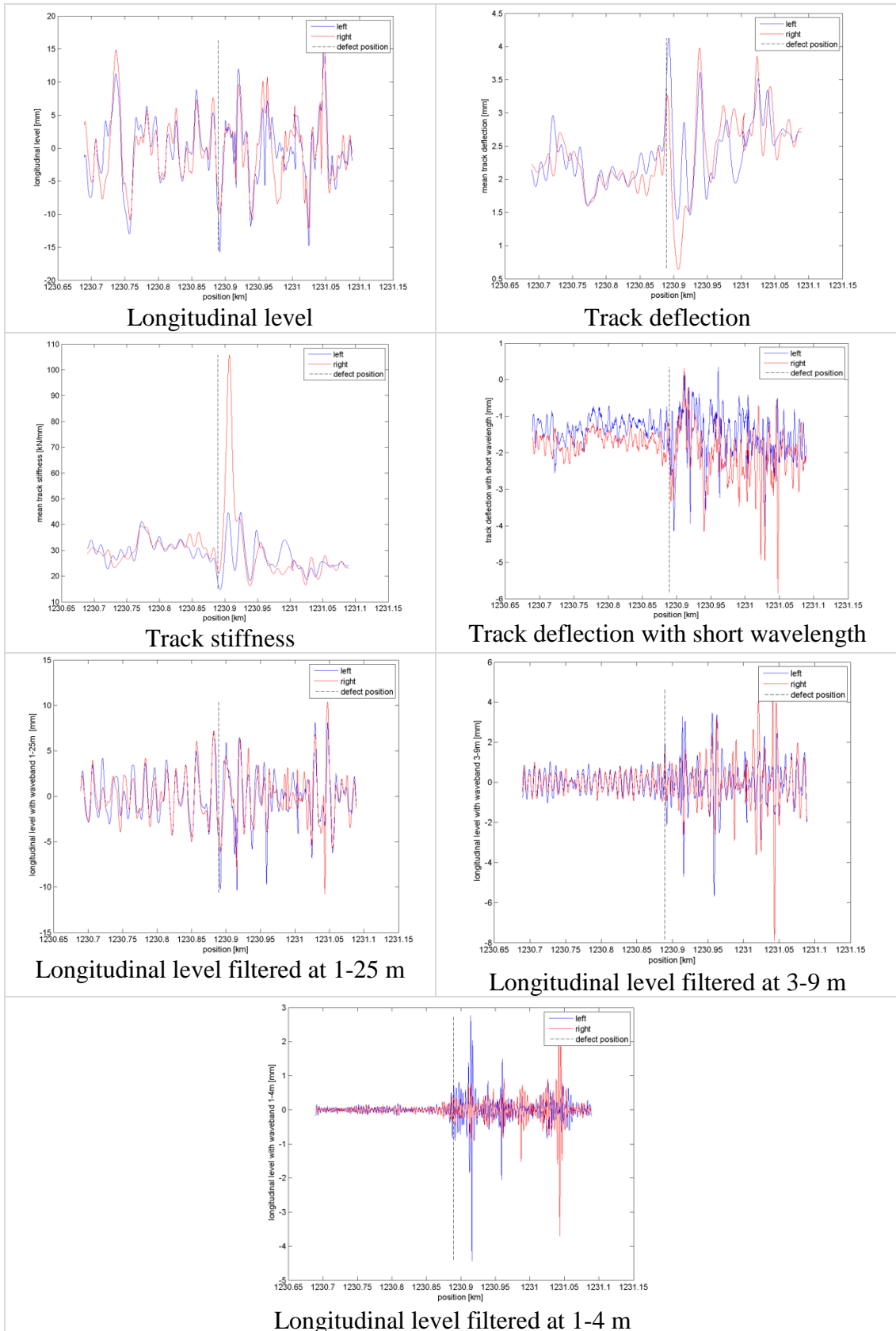
```

9.4 Track characteristics extracted from sample 1 for four detected defects

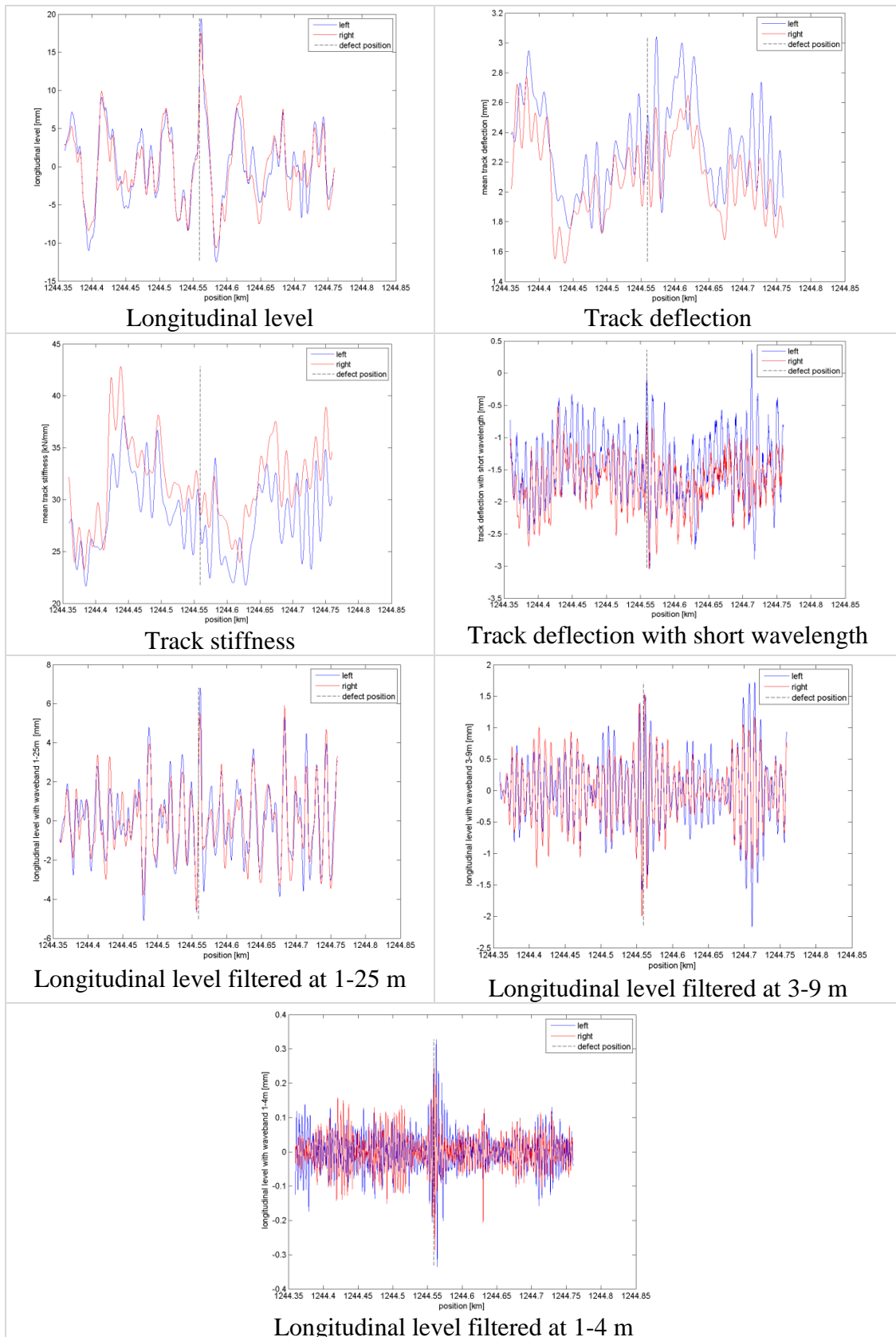
(1): Defect located at 1165.512 km



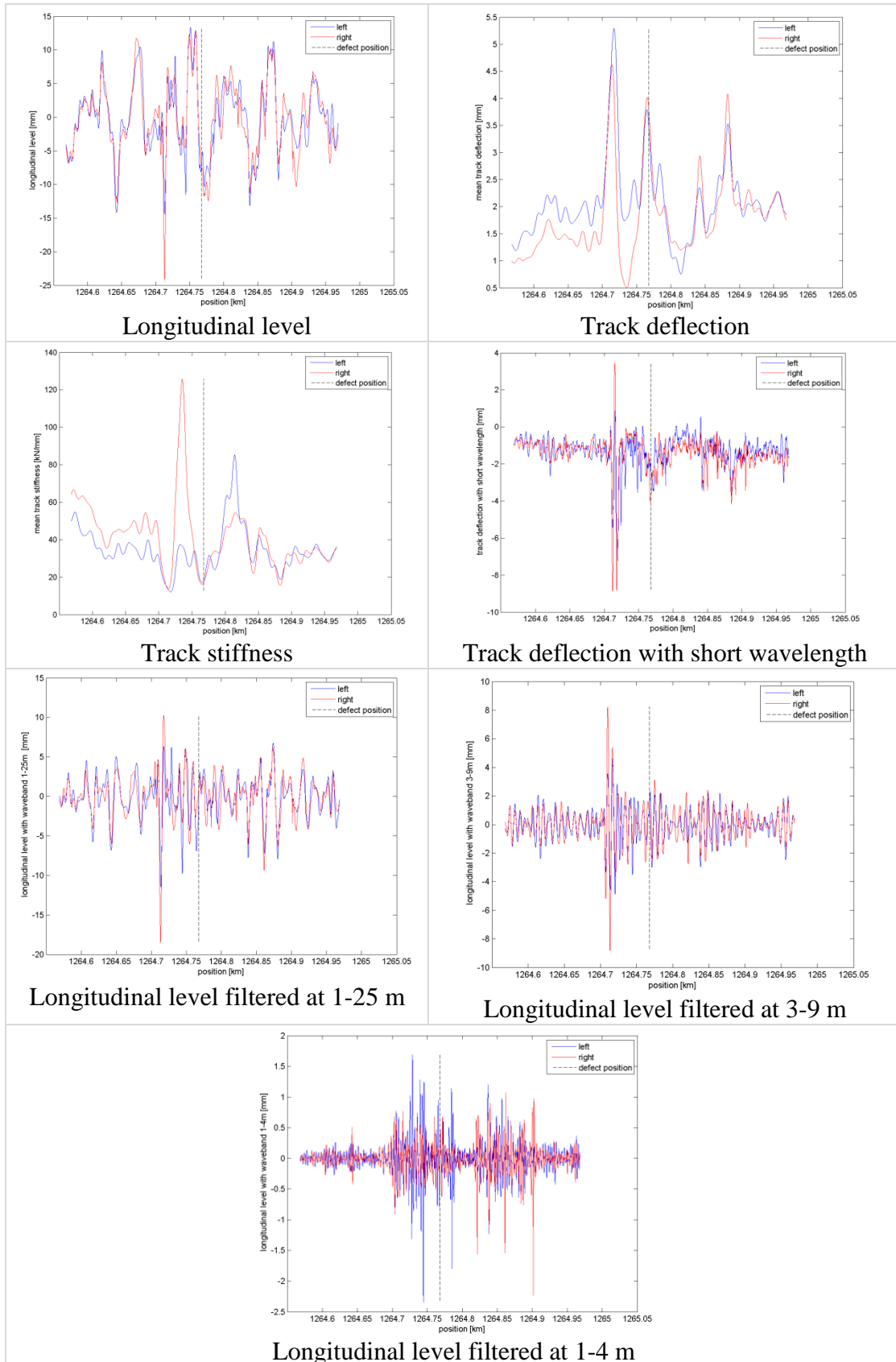
(2): Defect located at 1230.889 km



(3): Defect located at 1244.559 km



(4): Defect located at 1264.768



9.5 Track stiffness deviations of samples 2 to 5

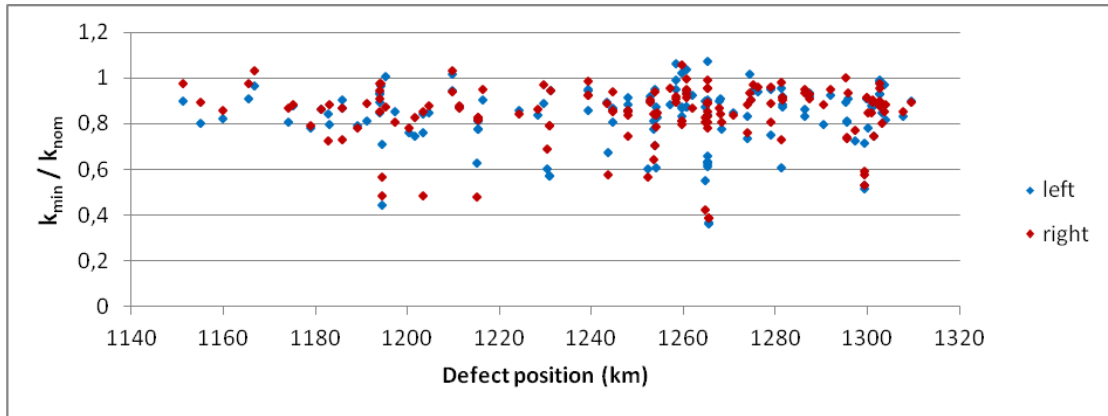


Figure 36: Minimum track stiffness over nominal stiffness for left rail and right rail with respect to defect positions for sample 2

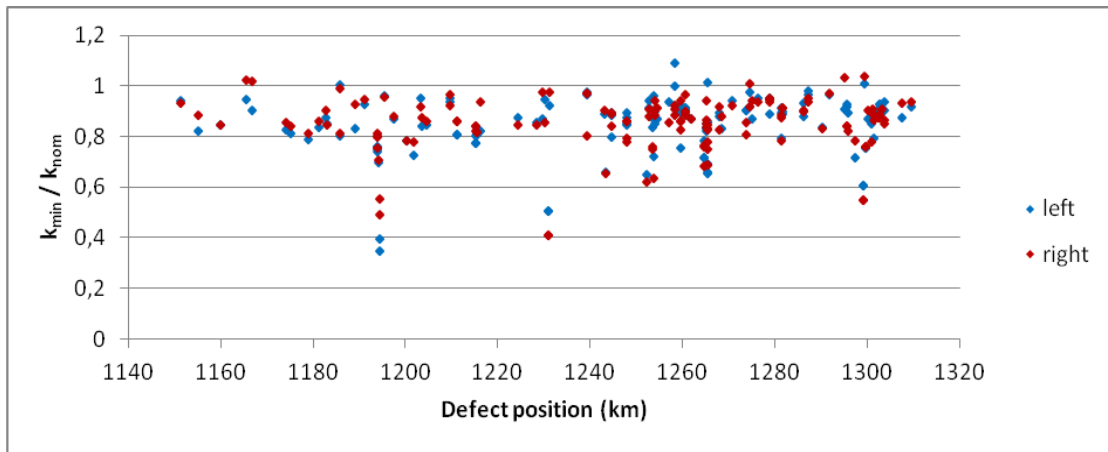


Figure 37 :Minimum track stiffness over nominal stiffness for left rail and right rail with respect to defect positions for sample 3

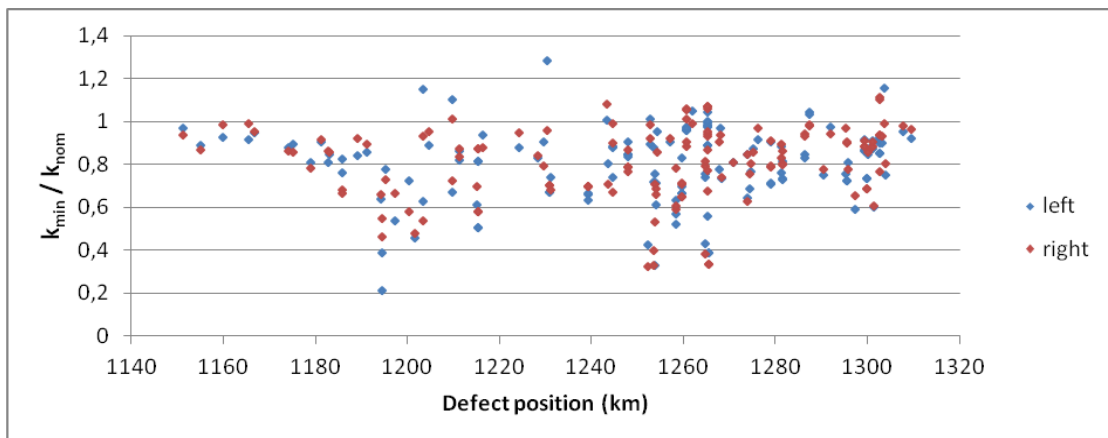


Figure 38: Minimum track stiffness over nominal stiffness for left rail and right rail with respect to defect positions for sample 4

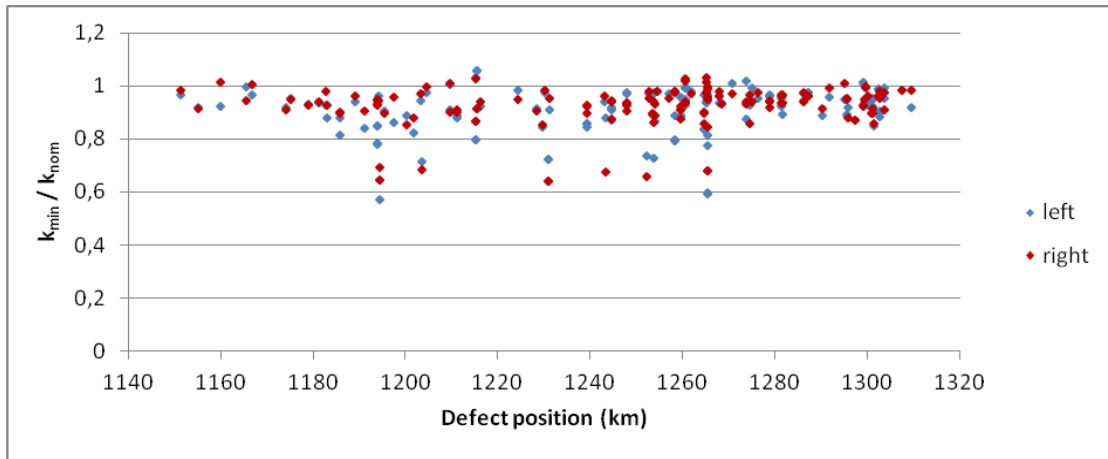


Figure 39 : Minimum track stiffness over nominal stiffness for left rail and right rail with respect to defect positions for sample 5

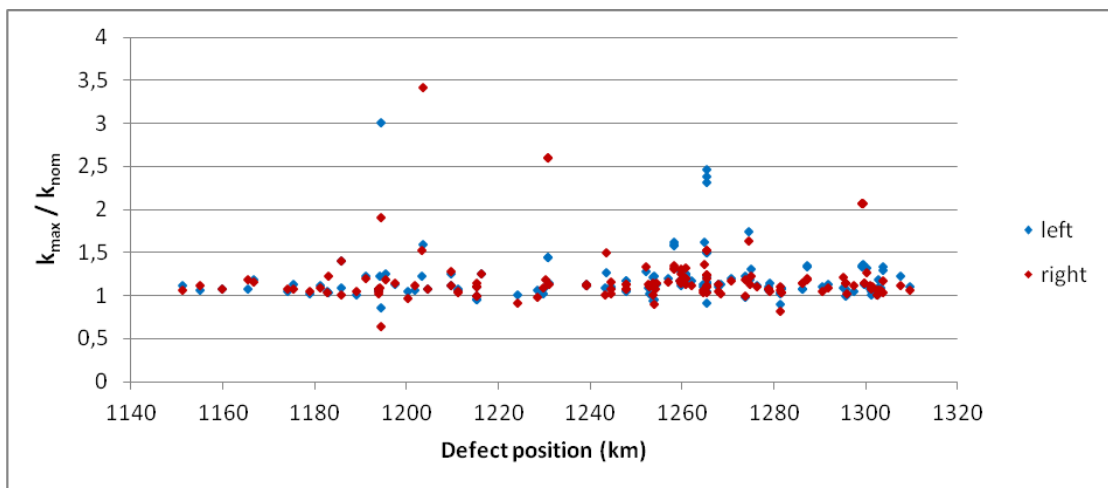


Figure 40: Maximum track stiffness over nominal stiffness for left rail and right rail with respect to defect positions for sample 2

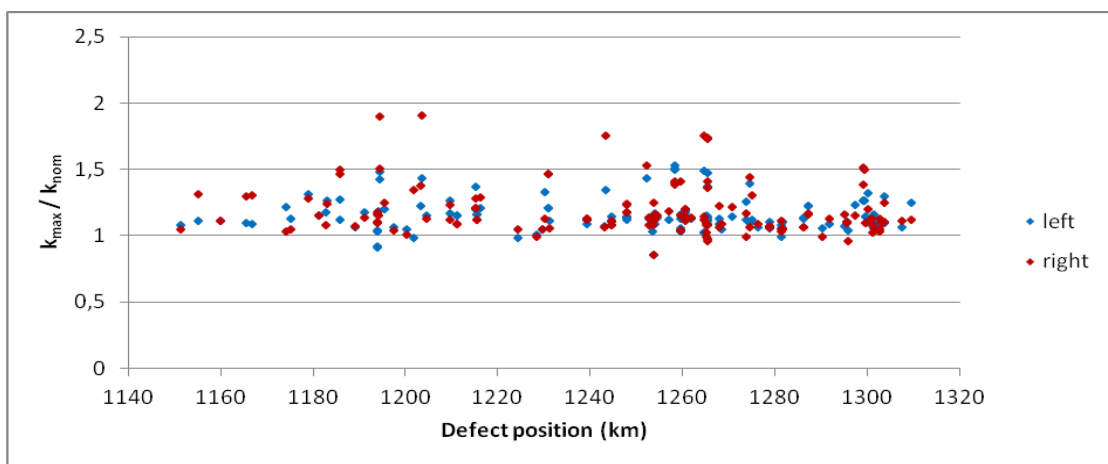


Figure 41: Maximum track stiffness over nominal stiffness for left rail and right rail with respect to defect positions for sample 3

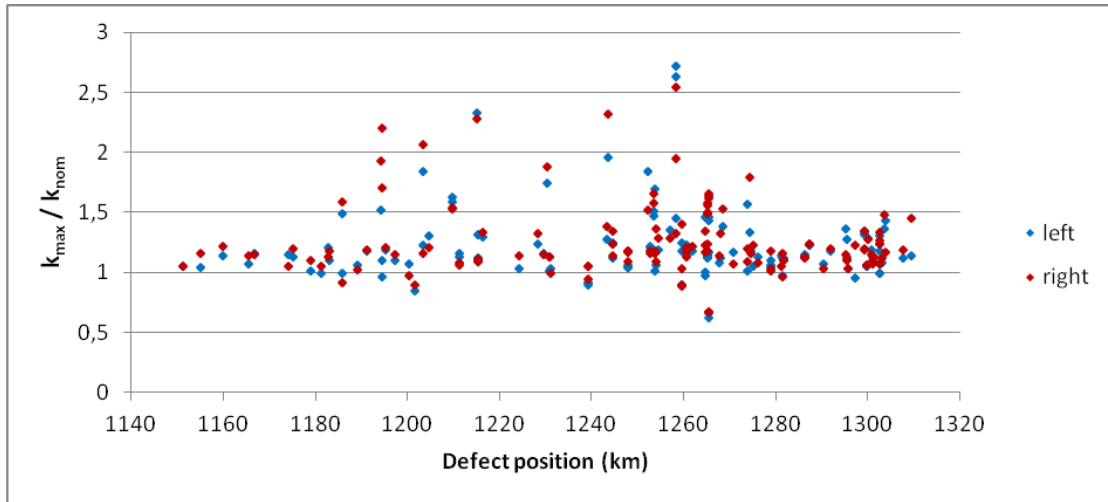


Figure 42: Maximum track stiffness over nominal stiffness for left rail and right rail with respect to defect positions for sample 4

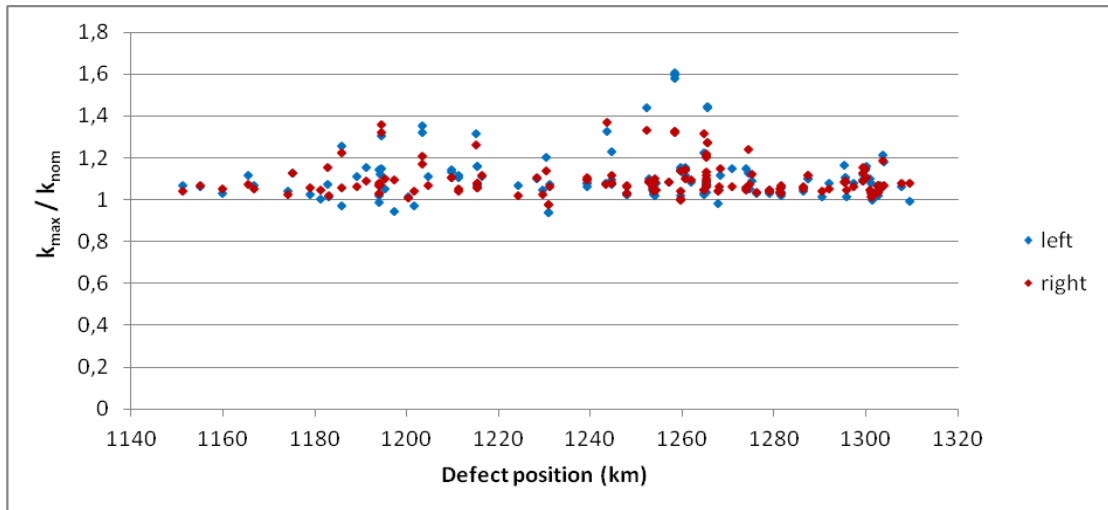


Figure 43: Maximum track stiffness over nominal stiffness for left rail and right rail with respect to defect positions for sample 5

9.6 Deviations of deflection with short wavelength content of samples 2 to 5

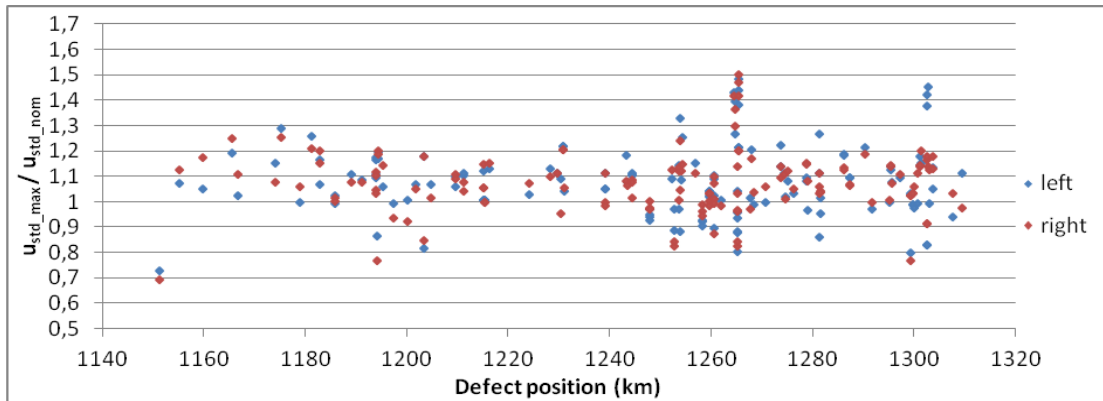


Figure 44 – Maximum swept standard deviation over nominal swept standard deviation of filtered deflection for left rail and right rail with respect to defect positions for sample 2

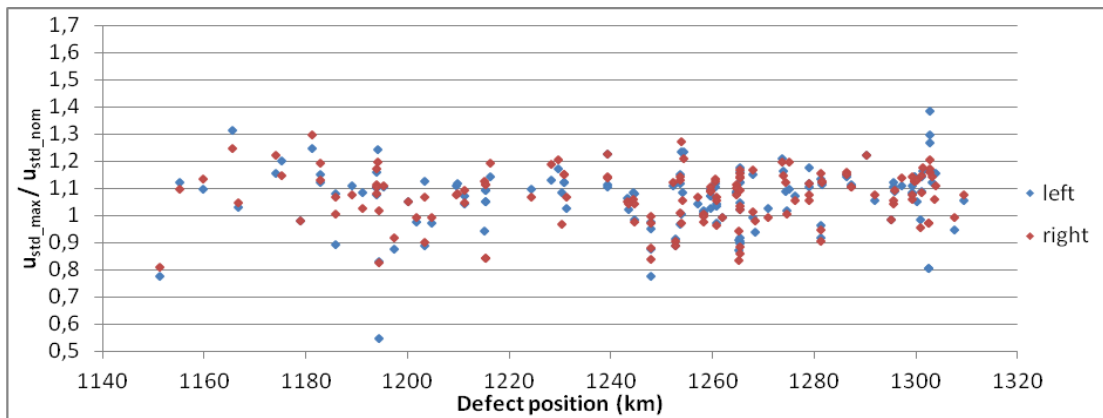


Figure 45 - Maximum swept standard deviation over nominal swept standard deviation of filtered deflection for left rail and right rail with respect to defect positions for sample 3

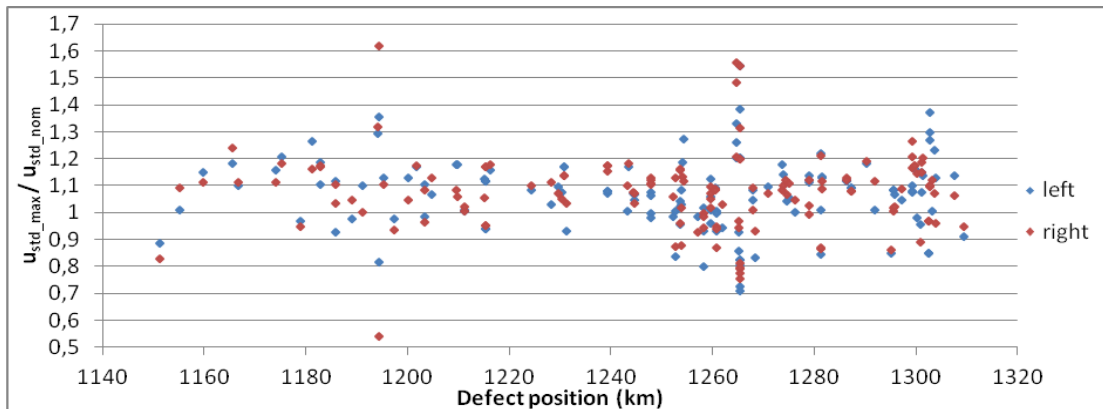


Figure 46 - Maximum swept standard deviation over nominal swept standard deviation of filtered deflection for left rail and right rail with respect to defect positions for sample 4

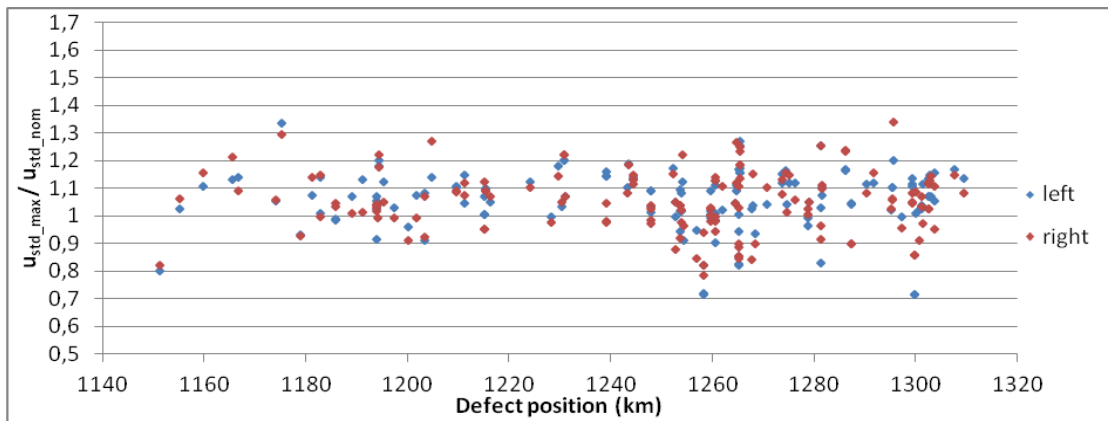


Figure 47 - Maximum swept standard deviation over nominal swept standard deviation of filtered deflection for left rail and right rail with respect to defect positions for sample 5

9.7 Maximum and minimum bending moments along the rail considering several hanging sleepers

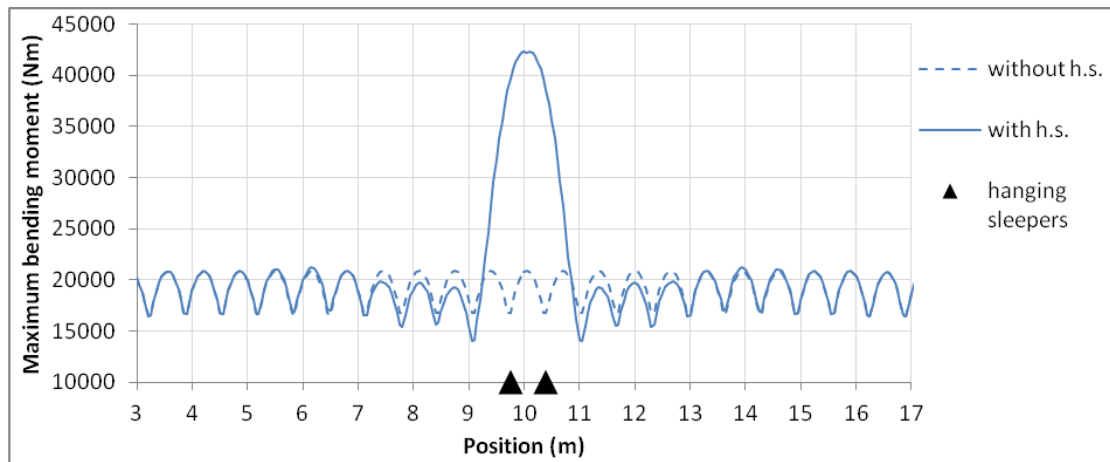


Figure 48 - Maximum bending moment considering two consecutive hanging sleepers, compared to a case without hanging sleepers

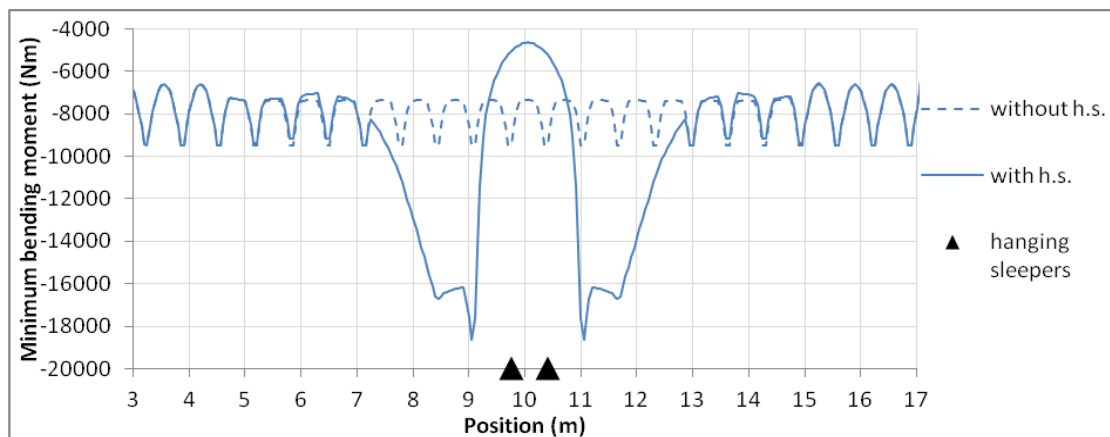


Figure 49 - Minimum bending moment considering two consecutive hanging sleepers, compared to a case without hanging sleepers

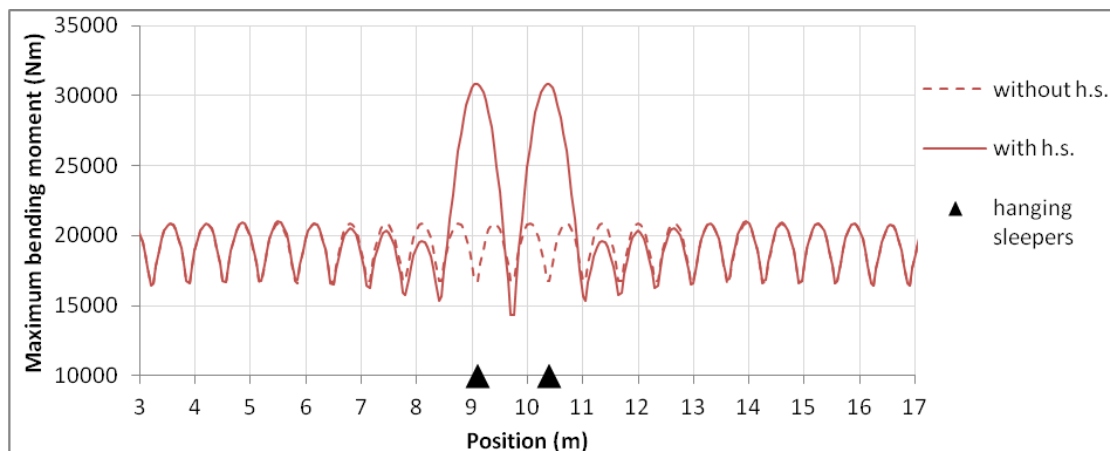


Figure 50 - Maximum bending moment considering two hanging sleepers separated by a normal sleeper, compared to a case without hanging sleepers

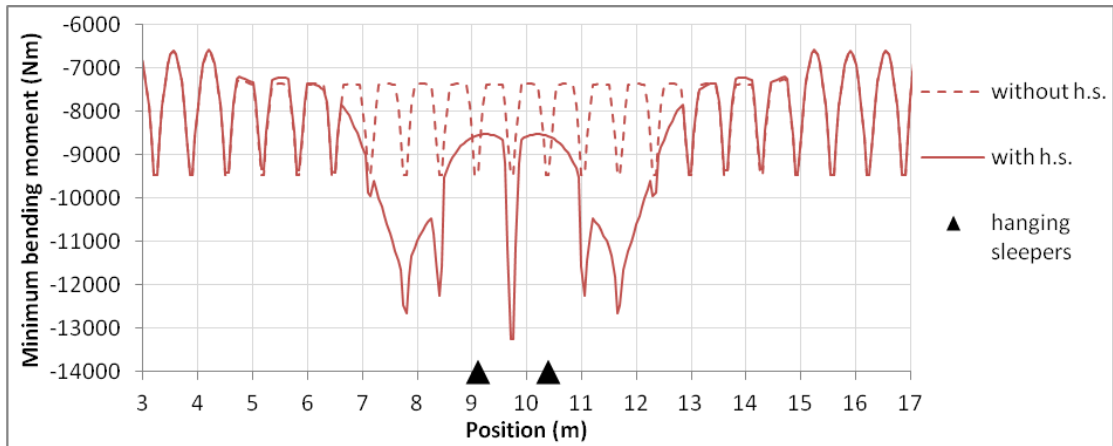


Figure 51 - Minimum bending moment considering two hanging sleepers separated by a normal sleeper, compared to a case without hanging sleepers

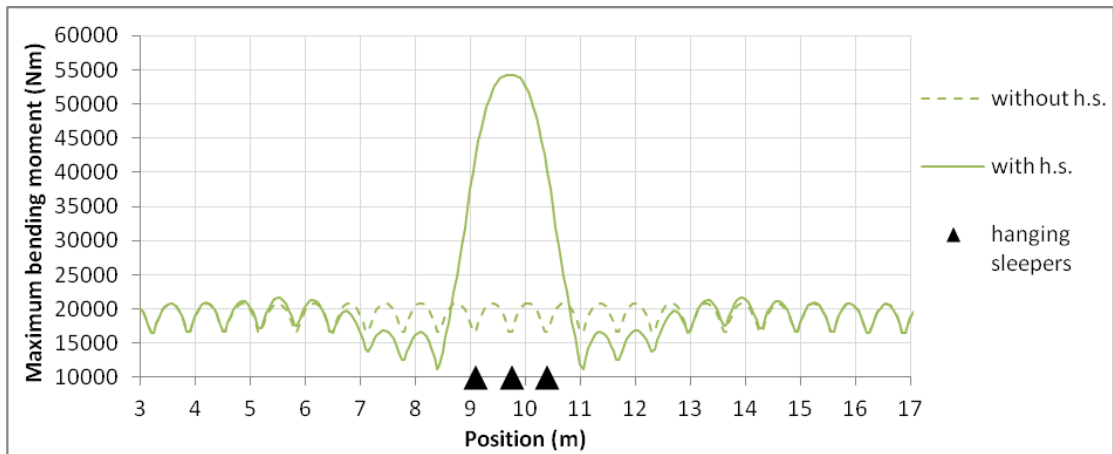


Figure 52 - Maximum bending moment considering three hanging sleepers, compared to a case without hanging sleepers

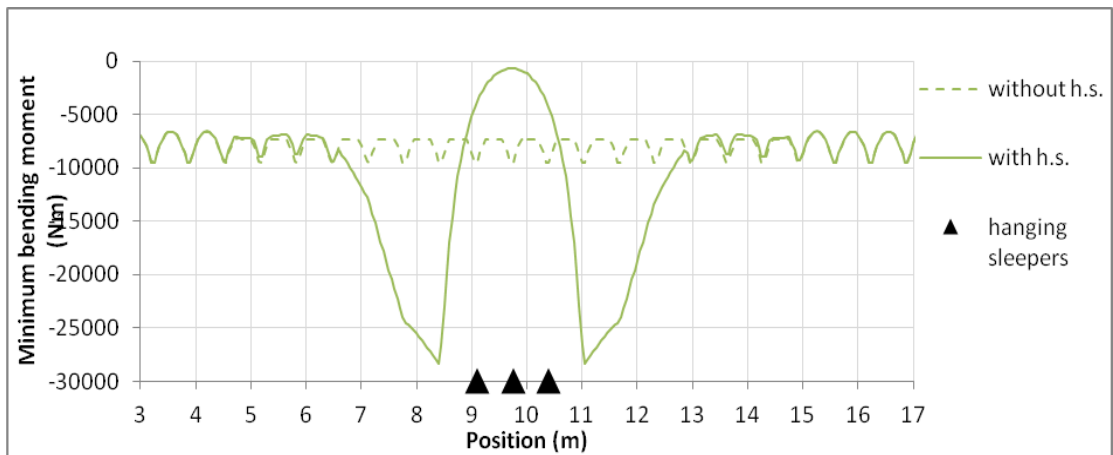


Figure 53 - Minimum bending moment considering three hanging sleepers, compared to a case without hanging sleepers

9.8 Maximum and minimum bending moments along the rail with different loads and nominal stiffness

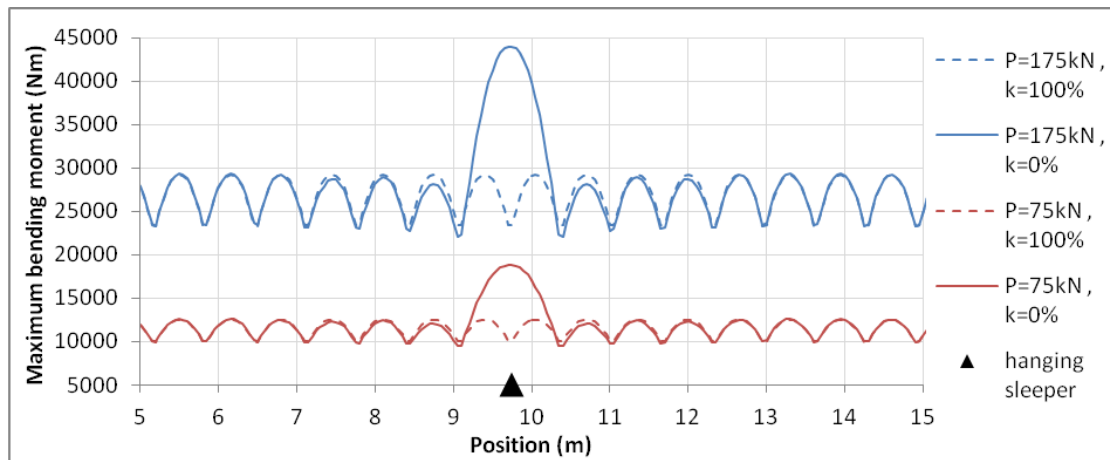


Figure 54 - Maximum bending moment for cases with and without a hanging sleeper ($k=0\%$ and $k=100\%$, respectively), for different loads

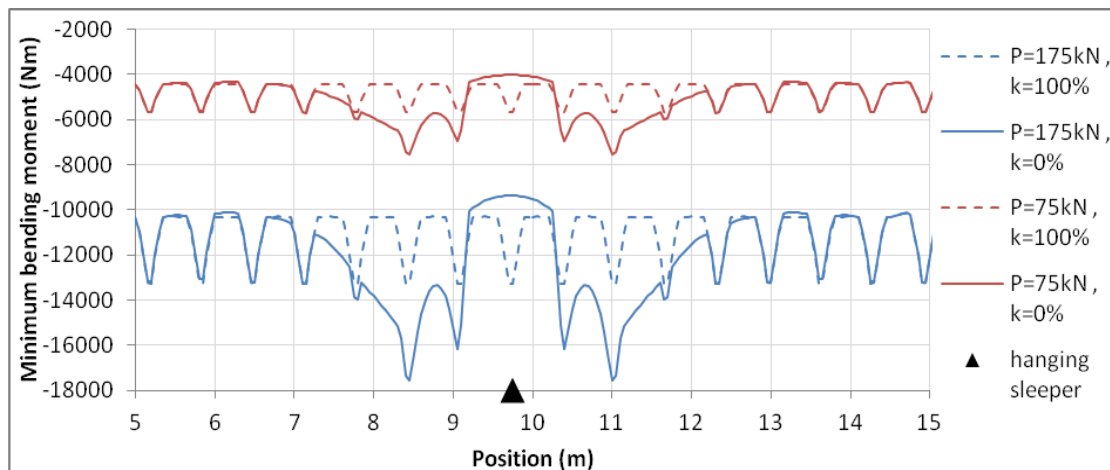


Figure 55 - Minimum bending moment for cases with and without a hanging sleeper ($k=0\%$ and $k=100\%$, respectively), for different loads

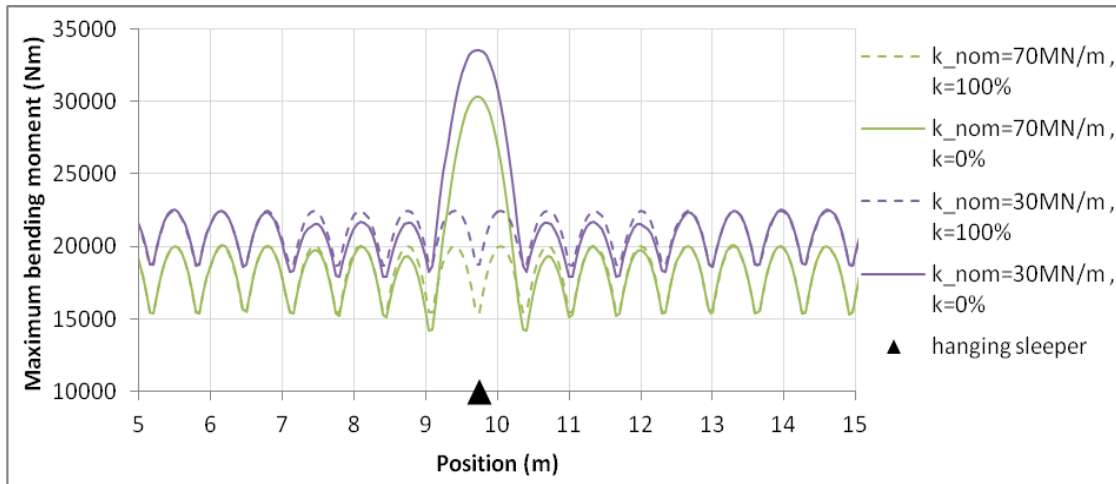


Figure 56 - Maximum bending moment for cases with and without a hanging sleeper ($k=0\%$ and $k=100\%$, respectively), for different nominal stiffness magnitudes

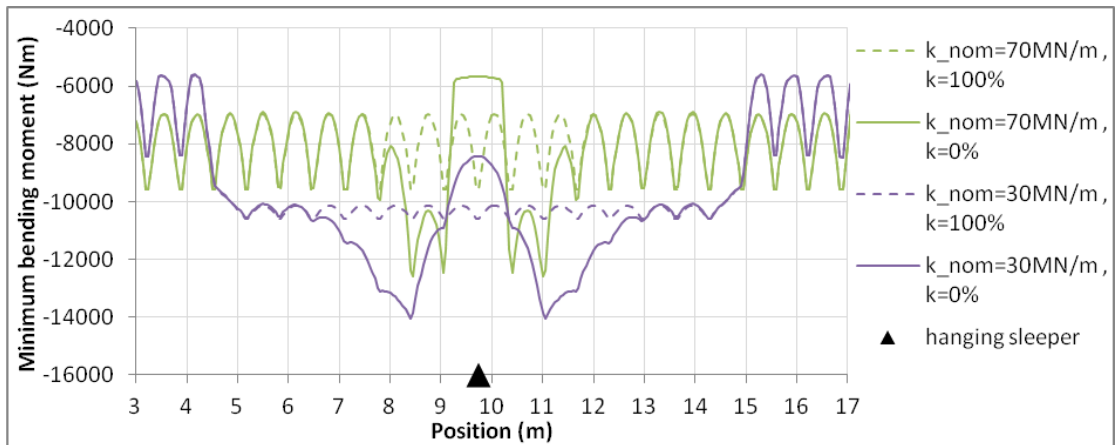


Figure 57 - Minimum bending moment for cases with and without a hanging sleeper ($k=0\%$ and $k=100\%$, respectively), for different stiffness magnitudes